arXiv:cond-mat/0412225v2 [cond-mat.stat-mech] 15 Mar 2005

Three-body problem for ultracold atoms in quasi-one-dimensional traps

C. Mora,[1] R. Egger,[1] and A.O. Gogolin[2]
[1] *Institut für Theoretische Physik, Heinrich-Heine-Universität, D-40225 Düsseldorf, Germany*
[2] *Department of Mathematics, Imperial College London, 180 Queen's Gate, London SW7 2AZ, United Kingdom*
(Dated: March 23, 2022)

We study the three-body problem for both fermionic and bosonic cold atom gases in a parabolic transverse trap of lengthscale $a_\perp$. For this quasi-one-dimensional (1D) problem, there is a two-body bound state (dimer) for any sign of the 3D scattering length a, and a confinement-induced scattering resonance. The fermionic three-body problem is universal and characterized by two atom-dimer scattering lengths, a_{ad} and b_{ad}. In the tightly bound 'dimer limit', $a_\perp/a \to \infty$, we find $b_{ad} = 0$, and a_{ad} is linked to the 3D atom-dimer scattering length. In the weakly bound 'BCS limit', $a_\perp/a \to -\infty$, a connection to the Bethe Ansatz is established, which allows for exact results. The full crossover is obtained numerically. The bosonic three-body problem, however, is non-universal: a_{ad} and b_{ad} depend both on $a_\perp/a$ and on a parameter R^* related to the sharpness of the resonance. Scattering solutions are qualitatively similar to fermionic ones. We predict the existence of a single confinement-induced three-body bound state (trimer) for bosons.

PACS numbers: 03.75.Ss, 05.30.Fk, 03.65.Nk

I. INTRODUCTION

The physics of cold atoms has recently enjoyed a great amount of attention. A particularly interesting phenomenon in that context has been the experimental observation of dimer (molecule) formation in ultracold binary Fermi gases [1], where a Feshbach resonance is exploited. This has allowed experimental access to the full crossover from a Bose-Einstein condensate (BEC) to a BCS-type superfluid by simply tuning a magnetic field [2, 3, 4, 5, 6]. Because of the Feshbach-resonant behavior, the 3D scattering length a describing the s-wave interaction strength among different fermions can be tuned almost at will. For $a > 0$, one has a two-body bound state ('dimer') that eventually can be Bose-condensed, while for $a < 0$, Cooper pairs are formed. The corresponding BEC-BCS crossover theory has been worked out on a mean-field (plus fluctuations) level [7, 8, 9, 10], and is widely believed to account for the basic experimental observations [11]. The Feshbach resonance has also interesting implications for bosonic systems, e.g., the existence of a similar crossover from atomic BEC to molecular BEC [12, 13, 14], or Bose-enhanced 'quantum superchemistry' [15, 16].

A related but different quasi-1D problem arises for either a two-species $(\uparrow,\downarrow)$ Fermi gas or a single-species Bose gas. When such a cold atom gas is confined to a sufficiently tight harmonic transverse trap, it enters a 1D regime. On the two-body level, there is always a bound state, even for $a < 0$, and one has a confinement-induced resonance (CIR) in the 1D atom-atom scattering length a_{aa} [17, 18]. This 'shape' (or 'geometric') resonance is similar to a Feshbach resonance [19]. Instead of a magnetic field, the ratio $a/a_\perp$ between the 3D scattering length and the transverse confinement lengthscale $a_\perp$, see Eq. (1.2) below, is now used to sweep through the resonance. Albeit there are strong quantum fluctuations in 1D, preventing both BEC and a true BCS superfluid in the thermodynamic limit, the presence of the CIR leads to a rather similar scenario as for the standard (3D) BEC-BCS crossover [20, 21, 22]. Moreover, this 1D analogue of the 3D BEC-BCS crossover and its bosonic complement appear to be experimentally feasible. Recent progress towards the realization of 1D traps has been tremendous [23, 24, 25, 26, 27] and could lead to the observation of interesting aspects of 1D many-body physics as outlined below. Moreover, on the theoretical side, powerful many-body techniques are available in 1D systems, e.g., bosonization [28], or the Bethe Ansatz [29, 30]. Such methods often allow for exact statements. Below we analytically solve the three-body problem for ultracold fermions or bosons that are confined to quasi-1D by a transverse trap potential. We show that, for low energies, atom-dimer scattering solutions can be completely described in terms of two scattering lengths a_{ad} and b_{ad}, where a_{ad} can be linked to the standard 3D atom-dimer scattering length. The non-standard scattering length b_{ad} must be introduced to describe 1D scattering processes in general. While the (fermionic and bosonic) three-body problem in 3D systems has a rather long history, reviewed in Refs. [19, 31], the quasi-1D situation has not received much attention so far.

In what follows, we assume two different hyperfine states of a fermion species of mass m_0, or a single boson species, to be trapped in the parabolic transverse confinement potential

$$U_c(\mathbf{r}) = \frac{1}{2} m_0 \omega_\perp^2 (x^2 + y^2), \tag{1.1}$$

with associated confinement lengthscale

$$a_\perp = \sqrt{2\hbar/m_0\omega_\perp}. \tag{1.2}$$

For a non-parabolic potential, the treatment is more involved [32], and new effects appear, e.g., additional reso-

nances. Under the standard pseudopotential approximation [33], for the low-energy limit of interest here, the 3D interaction can be written as

$$V(\mathbf{r}) = \frac{4\pi\hbar^2 a}{m_0}\delta(\mathbf{r})\frac{\partial}{\partial r}(r\cdot), \tag{1.3}$$

which assumes that the interaction range is the shortest lengthscale of relevance in the problem. On the two-body level, interactions between atoms are thereby described in terms of the 3D scattering length a. Normally, at low energy scales only s-wave interactions matter. Identical fermions then do not interact because of the Pauli principle, but interactions among different ones will be present and are given by Eq. (1.3). The free (unconfined) problem is well-known to possess exactly one bound state ('dimer') on the two-body level for $a > 0$ [34]. Once the confinement (1.1) is present, however, there is *always* a two-body bound state with dimensionless binding energy

$$\Omega_B = (\hbar\omega_\perp - E_B)/2\hbar\omega_\perp = (\kappa_B a_\perp/2)^2, \tag{1.4}$$

where $a_B = 1/\kappa_B$ is the (longitudinal) size of the dimer. This quantity is determined by the condition [17, 18]

$$\zeta(1/2, \Omega_B) + a_\perp/a = 0. \tag{1.5}$$

For our purposes, the Hurvitz zeta function can be defined via its integral representation (see appendix A),

$$\zeta(1/2, \Omega) = \int_0^\infty \frac{dt}{\sqrt{\pi t}}\left(\frac{e^{-\Omega t}}{1-e^{-t}} - \frac{1}{t}\right). \tag{1.6}$$

Since $\zeta(1/2, \Omega)$ is monotonic in Ω, there is precisely one bound state for any given $a_\perp/a$. This bound-state wavefunction can then be expressed in terms of the single-particle Green's function $G_E(\mathbf{r}, \mathbf{r}')$ for the cylindrical harmonic oscillator with reduced mass $m_0/2$, see Eqs. (2.14) and (2.15) below. For $a_\perp/a \to -\infty$, the 'BCS limit' is reached, where $\Omega_B \simeq (a/a_\perp)^2 \ll 1$. (For simplicity, we shall use the phrase 'BCS limit' also for bosons, even though there is no Cooper pairing in that case.) The dimer is then very elongated, with size $a_B \approx a_\perp^2/|a| \gg a_\perp$ in the axial direction, and confined to the transverse ground state. The dimer in this limit can be effectively described by a 1D contact interaction obtained by projecting the pseudopotential (1.3) to the lowest transverse state. In the tightly bound 'dimer limit', $a_\perp/a \to +\infty$, the dimer becomes spherically symmetric with the size $a_B \approx a \ll a_\perp$. Here, one recovers the pseudopotential bound state of the unconfined problem (for $a > 0$) with the large reduced binding energy $\Omega_B \simeq (a_\perp/2a)^2 \gg 1$.

The analogue of the Feshbach resonance in a 1D confined system is then realized by the CIR. Solving the two-body scattering problem with just one open channel, the 1D scattering length between two atoms can be extracted and is found to be [17, 18]

$$a_{aa} = -\frac{a_\perp}{2}\left[\frac{a_\perp}{a} - \mathcal{C}\right], \quad \mathcal{C} = -\zeta(1/2) \simeq 1.4603. \tag{1.7}$$

At low energies, this implies that one can use the 1D atom-atom interaction potential

$$V_{aa}(z, z') = g_{aa}\delta(z - z'), \quad g_{aa} = -\frac{2\hbar^2}{m_0 a_{aa}}. \tag{1.8}$$

The CIR, where $g_{aa} \to \pm\infty$, then occurs for $a_{aa} = 0$, corresponding to $\Omega_B = 1$, and can be reached by tuning $a_\perp$ or a. The physical picture behind the emergence of the resonance has been elucidated in Ref. [18] and shown to be similar to a Feshbach resonance. Atoms in the lowest transverse level (open channel) are coupled resonantly to a bound state in the two-body sector restricted to excited channels (closed channel). This picture has also recently been extended to non-parabolic potentials [32]. Although up to now, no clear experimental evidence for CIR behavior has been published, there are several possibilities to observe it using standard techniques, e.g., via the momentum distribution or Bragg spectroscopy.

The above considerations suggest that it is mandatory to analyze the consequences of this CIR on the many-body scattering properties [20, 21]. As a first step towards a full understanding of this problem, we discuss the analytic solution of the corresponding three-body problem, which here becomes possible due to the short-rangedness of the atom-atom interaction. A natural question then concerns the scattering properties of the atom-dimer system, for instance, the scattering length a_{ad}. For fermions, this problem has been solved already a long time ago by Skorniakov and Ter-Martirosian (STM) [35], who found $a_{ad} \approx 1.2a$. (This result was recovered recently [36] as a particular limit for different masses of the two fermion species.) One may then wonder whether atom-dimer scattering will also show resonance enhancement, whether three-body physics remains universal (i.e., determined by two-body quantities only), and whether a three-body bound state ('trimer') is possible. We find that in the fermionic case (with equal masses), the low-energy physics is universal like in the 3D case [37], and there is no trimer state. However, in the bosonic case, important differences to these answers for fermions can and do arise.

At this point, we pause in order to briefly discuss the bosonic three-body problem in 3D [19]. It was shown by Thomas in 1935 [38] that there is no lower bound on the energy of a system of three bosons interacting via zero-range forces ('Thomas collapse'). The corresponding integral equation for the scattering amplitude was derived by STM [35], but in Ref. [39] it was shown that their equation is not well-defined, since it allows for an infinite number of solutions. A scheme of choosing the correct solution based on the orthogonality of wavefunctions with different energies was suggested. A related equation for the bound states was investigated in Ref. [40], where an infinite number of three-body bound states with arbitrarily low energies was found. Furthermore, in the unitary limit $a \to \infty$, bound states condense at the continuum threshold. The condition of Ref. [39] was identified as a self-adjoint extension of the involved operator.

Finally, Efimov solved the problem [37] by introducing a three-body short-distance parameter. Away from the unitary limit, there is at most a finite number of bound states ('Efimov states'), but in the unitary limit a peculiar hierarchy of infinitely many bound states emerges [19, 37]. This regularization also affects the scattering solution. To summarize, the 3D integral equations for bosons generally require both a long-distance cutoff (the scattering length a) and a short-distance cutoff. Efimov's real-space implementation of the short-distance cutoff is not very convenient for the confined problem. Fortunately, Petrov [41] recently suggested a different and in the present context more useful regularization based on the energy dependence of the scattering length,

$$a^{-1} \to a^{-1} + R^* m_0 E_c/\hbar^2, \tag{1.9}$$

evaluated at the collision energy E_c of the atom-dimer complex, i.e., the total energy minus the (kinetic and confinement) energy of the relative motion. Here R^* is a parameter related to the sharpness of the Feshbach resonance, appearing also in the effective range expansion for the 3D scattering amplitude [34],

$$f_{3D}(k) = -\frac{1}{a^{-1} + ik + R^* k^2}. \tag{1.10}$$

We shall use the regularization (1.9) in our discussion of the bosonic three-body problem. Although in strictly 1D systems, there is no Efimov physics [19], in the quasi-1D case of a confined gas under study here, Efimov states can and will be relevant in certain limits.

The tunability of the scattering length a in cold atom experiments is obtained by using Feshbach resonances. For distances on the order of the interatomic potential, the two-body problem is coupled resonantly to a bound molecular state involving different spin states (closed channel). For larger distances, there is nevertheless only a small admixture of this closed channel and the two-body scattering is essentially reproduced by a one-channel zero-range potential with the scattering amplitude (1.10), omitting the (small) background scattering length. We refer to Ref. [42] for more details. For fermions, we will assume that R^* does not appear in Eq. (1.10) under the condition that $kR^* \ll 1$. This implies in particular that $R^* \ll a_B$ and $R^* \ll a_\perp$.

The structure of this paper is as follows. In Sec. II, we derive an integral equation that determines the complete solution of the fermionic three-body problem. This integral equation can be solved explictly after projection to the transverse ground-state of the trap, as is discussed in Sec. III. The role of the higher transverse channels is then addressed in Sec. IV, where also explicit contact to previous work in the unconfined case [35, 36] is established. A brief account of some of these results for fermions has been given in Ref. [43]. The bosonic three-body problem is then studied in detail in Sec. V. In Sec. VI, we highlight the tight connections to the Bethe Ansatz existing in the BCS limit for fermions and bosons, and present exact results obtained from this link. Finally, we conclude in Sec. VII.

II. FERMIONIC THREE-BODY PROBLEM

In this section, we consider the fermionic three-body problem ($\uparrow\uparrow\downarrow$) with two identical fermions, where the 'spin' indicates two selected hyperfine states of the atom. We denote by $\mathbf{x_1}$ ($\mathbf{x_{2,3}}$) the position of the $\downarrow$ (the two $\uparrow$) particles, and perform an orthogonal transformation to variables $(\mathbf{x}, \mathbf{y}, \mathbf{z})$ in order to decouple the center-of-mass coordinate $\mathbf{z}$,

$$\begin{pmatrix} \mathbf{x} \\ \mathbf{y} \\ \mathbf{z} \end{pmatrix} = \begin{pmatrix} 2/\sqrt{3} & -1/\sqrt{3} & -1/\sqrt{3} \\ 0 & -1 & 1 \\ \sqrt{2/3} & \sqrt{2/3} & \sqrt{2/3} \end{pmatrix} \begin{pmatrix} \mathbf{x}_1 \\ \mathbf{x}_2 \\ \mathbf{x}_3 \end{pmatrix}. \tag{2.1}$$

For the harmonic confinement (1.1), the potential remains diagonal in the positions, and the Schrödinger equation reads

$$\left(-\frac{\hbar^2}{m_0} \nabla^2_{\mathbf{X}} + U_c(\mathbf{X}) - E \right) \Psi(\mathbf{X}) = -\sum_{\pm} V(\mathbf{r}_\pm) \Psi(\mathbf{X}), \tag{2.2}$$

where $\mathbf{X} = (\mathbf{x}, \mathbf{y})$ is a six-dimensional vector. With these definitions, the distances between the $\downarrow$ particle and each $\uparrow$ particle are

$$\mathbf{r}_\pm = \sqrt{3}\mathbf{x}/2 \pm \mathbf{y}/2 = \sin\theta\, \mathbf{x} \pm \cos\theta\, \mathbf{y}, \tag{2.3}$$

where we introduce the angle $\theta = \pi/3$ for notational convenience, see also Ref. [36], such that $\sin\theta = \sin(2\theta) = \sqrt{3}/2$ and $\cos\theta = -\cos(2\theta) = 1/2$. Equation (1.3) then allows to incorporate the interactions $V(\mathbf{r}_\pm)$ via boundary conditions imposed for vanishing distances between $\uparrow$ and $\downarrow$ atoms. For $\mathbf{r}_\pm \to 0$, this implies the singular behavior

$$\Psi(\mathbf{X}) \simeq \mp \frac{f(\mathbf{r}_{\perp,\pm})}{4\pi r_\pm} (1 - r_\pm/a), \tag{2.4}$$

where the vectors $\mathbf{r}_{\perp,\pm} = \cos\theta\, \mathbf{x} \mp \sin\theta\, \mathbf{y}$ are orthogonal to $\mathbf{r}_\pm$, respectively. Since the pseudopotential (1.3) acts on Ψ according to

$$-\frac{m_0}{\hbar^2} V(\mathbf{r}_\pm) \Psi(\mathbf{X}) = \mp f(\mathbf{r}_{\perp,\pm}) \delta(\mathbf{r}_\pm),$$

the Schrödinger equation (2.2) becomes

$$\begin{aligned} \left(-\frac{\hbar^2}{m_0} \nabla^2_{\mathbf{X}} + U_c(\mathbf{X}) - E \right) \Psi(\mathbf{X}) &= \sum_{\pm} \mp \frac{\hbar^2 f(\mathbf{r}_{\perp,\pm})}{m_0} \delta(\mathbf{r}_\pm) \\ &= S(\mathbf{x}, \mathbf{y}). \end{aligned} \tag{2.5}$$

Now we introduce the two-particle Green's function

$$G^{(2)}_E(\mathbf{r}_1, \mathbf{r}_2; \mathbf{r}_3, \mathbf{r}_4) = \sum_{\lambda_1, \lambda_2} \frac{\psi_{\lambda_1}(\mathbf{r}_1) \psi_{\lambda_2}(\mathbf{r}_2) \psi^*_{\lambda_1}(\mathbf{r}_3) \psi^*_{\lambda_2}(\mathbf{r}_4)}{E_{\lambda_1} + E_{\lambda_2} - E}, \tag{2.6}$$

where ψ_λ denotes the eigenfunctions to the single-particle problem (for reduced mass $m_0/2$) with eigenenergy E_λ. The quantum numbers λ include the longitudinal (1D) momentum k, the integer angular momentum m, and the radial quantum number $n = 0, 1, 2\ldots$, whence

$$\begin{aligned} E_\lambda &= \hbar\omega_\perp(2n + |m| + 1) + \hbar^2 k^2/m_0 \\ \psi_\lambda &= e^{im\phi} R_{nm}(\rho) e^{ikz} \end{aligned} \tag{2.7}$$

with radial functions [see also Eq. (1.2)]

$$\begin{aligned} R_{nm}(\rho) \;&=\; \frac{1}{\sqrt{\pi}\; a_\perp}\sqrt{n!/(n+|m|)!} \\ &\times\; (\rho/a_\perp)^{|m|} L_n^{|m|}(\rho^2/a_\perp^2) e^{-\frac{1}{2}(\rho/a_\perp)^2}, \end{aligned} \tag{2.8}$$

where $L_n^m(x)$ denotes standard Laguerre polynomials. Using Eq. (2.6), the general solution of Eq. (2.5) can be expressed as

$$\Psi(\mathbf{X}) = \Psi_0(\mathbf{X}) + \int d\mathbf{x}' d\mathbf{y}' G_E^{(2)}(\mathbf{x},\mathbf{y};\mathbf{x}',\mathbf{y}') S(\mathbf{x}',\mathbf{y}'), \tag{2.9}$$

where $\Psi_0(\mathbf{X})$, only present for positive energy E, is a homogeneous (free) solution. In this paper, we restrict our attention to states with $E < 0$, such that $\Psi_0 = 0$, and write

$$E = -2\Omega_B\, \hbar\omega_\perp + \hbar^2 \bar{k}^2/m_0, \tag{2.10}$$

where the relative momentum $\bar{k}$ of the atom-dimer complex is sent to zero later.

Since $S(\mathbf{x},\mathbf{y})$ in Eq. (2.9) involves the variables $\mathbf{r}_{\perp,\pm}$ and $\mathbf{r}_\pm$, see Eq. (2.5), it is advantageous to switch to these by virtue of the orthogonal transformation

$$\begin{pmatrix} \mathbf{r}_\pm \\ \mathbf{r}_{\perp,\pm} \end{pmatrix} = \begin{pmatrix} \sin\theta & \pm\cos\theta \\ \cos\theta & \mp\sin\theta \end{pmatrix} \begin{pmatrix} \mathbf{x} \\ \mathbf{y} \end{pmatrix}. \tag{2.11}$$

Similarly, we can switch from $(\mathbf{r}_{\perp,-}, \mathbf{r}_-)$ to $(\mathbf{r}_{\perp,+}, \mathbf{r}_+)$ using

$$\begin{pmatrix} \mathbf{r}_+ \\ \mathbf{r}_{\perp,+} \end{pmatrix} = \begin{pmatrix} -\cos 2\theta & \sin 2\theta \\ \sin 2\theta & \cos 2\theta \end{pmatrix} \begin{pmatrix} \mathbf{r}_- \\ \mathbf{r}_{\perp,-} \end{pmatrix}. \tag{2.12}$$

Since these are orthogonal transformations, $G_E^{(2)}$ stays invariant,

$$G_E^{(2)}(\mathbf{x},\mathbf{y};\mathbf{x}',\mathbf{y}') = G_E^{(2)}(\mathbf{r}_\pm, \mathbf{r}_{\perp,\pm}; \mathbf{r}'_\pm, \mathbf{r}'_{\perp,\pm}).$$

Furthermore, the integration measure in Eq. (2.9) is also invariant, $d\mathbf{x}'d\mathbf{y}' = d\mathbf{r}'_{\perp,\pm} d\mathbf{r}'_\pm$. We thus find from Eq. (2.9)

$$\begin{aligned} \frac{m_0}{\hbar^2}\,\Psi(\mathbf{r},\mathbf{r}_\perp) = \int d\mathbf{r}'_\perp\, f(\mathbf{r}'_\perp) \Big[& G_E^{(2)}(\mathbf{r},\mathbf{r}_\perp;0,\mathbf{r}'_\perp) \\ - \; & G_E^{(2)}\Big(-\cos(2\theta)\mathbf{r} + \sin(2\theta)\mathbf{r}_\perp, \sin(2\theta)\mathbf{r} + \cos(2\theta)\mathbf{r}_\perp; 0, \mathbf{r}'_\perp\Big)\Big], \end{aligned} \tag{2.13}$$

where $\mathbf{r} \equiv \mathbf{r}_-$ and $\mathbf{r}_\perp \equiv \mathbf{r}_{\perp,-}$. Next we implement the $\mathbf{r} \to 0$ limit according to Eq. (2.4) to obtain a closed equation for $f(\mathbf{r}_\perp)$. This limit can be directly taken for the non-singular second term in Eq. (2.13), while the first term contains the singular behavior necessary from Eq. (2.4). Once this singular behavior is removed, one obtains a regular integral equation for $f(\mathbf{r}_\perp)$ [35, 36].

It is then convenient to transform into the complete basis $\{\psi_\lambda\}$ specified above, $f(\mathbf{r}_\perp) = \sum_\lambda f_\lambda \psi_\lambda(\mathbf{r}_\perp)$. Notably, the last term in Eq. (2.13) can be expressed in terms of the single-particle Green's function

$$G_E(\mathbf{r},\mathbf{r}') = \sum_\lambda \frac{\psi_\lambda(\mathbf{r})\psi_\lambda^*(\mathbf{r}')}{E_\lambda - E}, \tag{2.14}$$

since

$$\begin{aligned} &\int d\mathbf{r}'_\perp\; G_E^{(2)}(\sin(2\theta)\mathbf{r}_\perp, \cos(2\theta)\,\mathbf{r}_\perp; 0, \mathbf{r}'_\perp) f(\mathbf{r}'_\perp) = \\ &\sum_\lambda G_{E-E_\lambda}(\sin(2\theta)\,\mathbf{r}_\perp, 0)\;\psi_\lambda(\cos(2\theta)\,\mathbf{r}_\perp)\;f_\lambda. \end{aligned}$$

The Green's function (2.14) for $\mathbf{r}' = 0$ has the integral representation

$$\begin{aligned} G_E(\mathbf{r},0) \;&=\; \frac{m_0}{4\pi\hbar^2 a_\perp}\int_0^\infty \frac{dt}{\sqrt{\pi t}}\frac{e^{-\Omega t}}{1-e^{-t}} \\ &\times\; \exp\left(-\frac{z^2}{a_\perp^2 t} - \frac{\rho^2}{2a_\perp^2}\coth(t/2)\right), \end{aligned} \tag{2.15}$$

where $\Omega = (\hbar\omega_\perp - E)/2\hbar\omega_\perp$. This can be obtained from the Feynman (imaginary-time) representation of the Green's function (2.14),

$$G_E(\mathbf{r},\mathbf{r}') = \int_0^\infty dt \sum_\lambda \psi_\lambda(\mathbf{r})\psi_\lambda^*(\mathbf{r}') e^{-t(E_\lambda - E)},$$

and the expressions for the eigenfunctions $\{\psi_\lambda\}$ and eigenenergies E_λ, see Eqs. (2.7) and (2.8), where only states with $m = 0$ contribute. One has to perform a straightforward gaussian integral over momenta k and the sum over n follows from the remarkable identity

$$\sum_{n=0}^\infty L_n^0\left(\frac{\rho^2}{a_\perp^2}\right) e^{-2n\hbar\omega_\perp t} = \frac{1}{1-e^{-2\hbar\omega_\perp t}} \exp\left(\frac{\rho^2}{a_\perp^2}\frac{e^{-2\hbar\omega_\perp t}}{e^{-2\hbar\omega_\perp t}-1}\right),$$

leading finally to Eq. (2.15). Using the orthonormality of the $\{\psi_\lambda\}$, the first term in the integral appearing in Eq. (2.13) can be written as

$$\begin{aligned} &\int d\mathbf{r}'_\perp G_E^{(2)}(\mathbf{r},\mathbf{r}_\perp;0,\mathbf{r}'_\perp) f(\mathbf{r}'_\perp) \\ &= \sum_{\lambda,\lambda_1} \frac{\psi_{\lambda_1}(\mathbf{r})\psi_{\lambda_1}^*(0)}{E_{\lambda_1} + E_\lambda - E}\psi_\lambda(\mathbf{r}_\perp) f_\lambda \\ &= \sum_\lambda G_{E-E_\lambda}(\mathbf{r},0)\psi_\lambda(\mathbf{r}_\perp) f_\lambda. \end{aligned} \tag{2.16}$$

For $\mathbf{r} \to 0$, the integral representation in Eq. (2.15) is dominated by small values of t. Its asymptotic behaviour

is then obtained by substracting and adding the leading term, such that

$$G_E(\mathbf{r},0) = \frac{m_0}{4\pi\hbar^2 a_\perp}\left(\int_0^\infty \frac{dt}{\sqrt{\pi}t^{3/2}} e^{-\Omega t - r^2/a_\perp^2 t} + \zeta(1/2,\Omega) + o(1)\right),$$

where the integral representation of the Hurvitz zeta function (1.6) has been used. Finally, performing the t integral, we find that for $\mathbf{r}\to 0$, Eq. (2.15) has the asymptotic behaviour $G_E(\mathbf{r},0) \simeq (m_0/4\pi\hbar^2 a_\perp)[a_\perp/r + \zeta(1/2,\Omega)]$. This implies that the leading term in Eq. (2.16) gives $m_0 f(\mathbf{r}_\perp)/(4\pi\hbar^2 r)$, which coincides with the singular part of $m_0\Psi(\mathbf{r},\mathbf{r}_\perp)/\hbar^2$ in the $r\to 0$ limit.

Using Eq. (2.4), and cancelling the $r\to 0$ singular terms in Eq. (2.13), straightforward algebra leads to an *integral equation* for $f(\mathbf{r})$. In the $\{\psi_\lambda\}$ representation, it reads

$$\mathcal{L}(\Omega_\lambda) f_\lambda = \sum_{\lambda'} A_{\lambda,\lambda'} f_{\lambda'}, \tag{2.17}$$

where we use the function, see also Eqs. (1.6) and (1.5),

$$\mathcal{L}(\Omega) = \zeta(1/2,\Omega) - \zeta(1/2,\Omega_B), \tag{2.18}$$

and the frequencies

$$\Omega_\lambda = \Omega_B - (a_\perp \bar{k}/2)^2 + E_\lambda/2\hbar\omega_\perp. \tag{2.19}$$

We find the kernel in the form

$$A_{\lambda\lambda'} = \frac{4\pi\hbar^2 a_\perp}{m_0}\int d\mathbf{r}_\perp\, \psi_\lambda^*(\mathbf{r}_\perp)\,\psi_{\lambda'}(\cos(2\theta)\mathbf{r}_\perp) \times G_{E-E_{\lambda'}}(\sin(2\theta)\mathbf{r}_\perp, 0). \tag{2.20}$$

In the following, it will be more convenient to use Ω_B instead of $a/a_\perp$ to parametrize the interaction strength, see Eq. (1.5).

Using Eq. (2.15), $A_{\lambda,\lambda'}$ can be evaluated explicitly, but before proceeding further, we shall perform a rescaling. Until now, f has only been considered as a function of the variable $\mathbf{r}_\perp = (\rho, z)$. However, in the asymptotic three-body scattering solution consisting of a dimer and one unbound atom, the atom-dimer distance $\mathbf{d}$ (which is then much bigger than the dimer size a_B) coincides with $\mathbf{r}_\perp$ only after a proper rescaling. The asymptotic solution is expected to be of the form

$$\Psi(\mathbf{r},\mathbf{r}_\perp) = \Phi_0(\mathbf{r})\chi(\mathbf{d}), \tag{2.21}$$

where $\mathbf{r}\equiv\mathbf{r}_-$ and the atom-dimer distance is

$$\mathbf{d} \equiv (\mathbf{x_1}+\mathbf{x_3})/2 - \mathbf{x_2} = \mathbf{r}_+ - \mathbf{r}_-/2.$$

Here $\Phi_0(\mathbf{r})$ is the wavefunction of the confinement-induced two-body bound state [17], and $\chi(\mathbf{d})$ gives the asymptotic solution for the scattering of the free particle by the dimer. The connection with f is made by looking at the $\mathbf{r}\to 0$ limit of Eq. (2.21). The leading term is

$$\Psi(\mathbf{r},\mathbf{r}_\perp) \simeq \frac{1}{4\pi r}\,\chi(\sin(2\theta)\mathbf{r}_\perp),$$

where we have used Eq. (2.12) to express $\mathbf{r}_+$ as a function of $\mathbf{r}$ and $\mathbf{r}_\perp$. In the asymptotic limit, $\sin(2\theta)\mathbf{r}_\perp$ is thus the atom-dimer distance. Therefore, after the rescaling $\mathbf{r}_\perp \to \sin(2\theta)\mathbf{r}_\perp$, the function f matches the asymptotic scattering solution χ. This length rescaling also implies wavevector rescaling, $k\to k/\sin(2\theta)$, as well as an extra factor $\sin(2\theta)$ in $A_{\lambda,\lambda'}$. In addition, from now on, we switch to dimensionless lengths and wavevectors by measuring them in units of $a_\perp$ and $1/a_\perp$, respectively.

III. LOWEST TRANSVERSE CHANNEL

Let us then proceed by projecting the integral equation (2.17) to the lowest transverse state ($n=m=0$). The role of the higher transverse channels will be discussed in Sec. IV. Taking into account the above rescaling, and noting that only $m=0$ modes have nonzero overlap with the lowest state,

$$\mathcal{L}(\Omega_k) f_k = \int_{-\infty}^{\infty}\frac{dk'}{2\pi} A_{k,k'} f_{k'}, \tag{3.1}$$

where

$$\Omega_k = \Omega_B + \sin^2(2\theta)(k^2 - \bar{k}^2)/4.$$

Straightforward algebra gives

$$A_{k,k'} = \sum_{p=0}^{\infty}\left(\frac{1+\cos(4\theta)}{2}\right)^p \times \frac{1}{p + \Omega_B + [k^2 + k'^2 + kk']/4 - 3\bar{k}^2/16}. \tag{3.2}$$

Note that the energy reads after the rescaling

$$E = -2\hbar\omega_\perp\Omega_B + \frac{3}{4}\frac{\hbar^2}{m_0}\left(\frac{\bar{k}}{a_\perp}\right)^2, \tag{3.3}$$

where $\bar{k}$ is interpreted as the relative momentum of a free particle with reduced mass $2m_0/3$.

A. Atom-dimer scattering solution

Following STM [35], we now make an *Ansatz* for the solution of this integral equation,

$$f(k) = 2\pi\delta(k-\bar{k}) + i\tilde{f}(k,\bar{k})\sum_{\pm}\frac{1}{\bar{k}\pm k + i0^+}, \tag{3.4}$$

with a *regular* function (scattering amplitude) $\tilde{f}(k,\bar{k})$. This Ansatz gives the expected asymptotic scattering state after Fourier transforming to real space,

$$f(z) = e^{i\bar{k}z} + \tilde{f}\left(\mathrm{sgn}(z)\bar{k},\bar{k}\right)e^{i\bar{k}|z|}, \qquad |z|\to+\infty,$$

such that standard transmission and reflection amplitudes [34] can be inferred,

$$t(\bar{k}) = 1 + \tilde{f}(\bar{k},\bar{k}), \quad r(\bar{k}) = \tilde{f}(-\bar{k},\bar{k}). \tag{3.5}$$

In the low-energy limit $k, \bar{k} \to 0$, the general expansion of the scattering amplitude applies,

$$\tilde{f}(k,\bar{k}) = -1 + ikb_{ad} + i\bar{k}a_{ad} + \mathcal{O}(k^2,\bar{k}^2,k\bar{k}). \tag{3.6}$$

Here a_{ad} and b_{ad} are the two 1D scattering lengths for the *atom-dimer scattering* process. In general, a_{ad} and b_{ad} are related to the even and odd partial scattered waves, respectively, as will be discussed in more detail in Sec. VI A. Let us just note at this point that for a sufficiently short-ranged potential, namely with support a_s smaller than the typical lengthscale for the wavefunction variations, the potential can be effectively described by a contact δ-interaction. This requires $a_s \ll |a_{ad}|$ and $\bar{k} \ll 1/a_s$. In that case, odd waves are not scattered by the potential and hence $b_{ad} = 0$ from Eq. (6.11). This is the case in particular for the two-body problem where only one scattering length, a_{aa} in Eq. (1.7), is usually given.

Inserting the Ansatz (3.4) into Eq. (3.1), we obtain

$$\begin{aligned}&\frac{\mathcal{L}(\Omega_k)}{\bar{k}^2-k^2}2i\bar{k}\tilde{f}(k,\bar{k}) - i\mathcal{P}\sum_{\pm}\int_{-\infty}^{\infty}\frac{dk'}{2\pi}\frac{A_{k,k'}}{\bar{k}\pm k'}\tilde{f}(k',\bar{k})\\ &-\frac{1}{2}\left[\tilde{f}(\bar{k},\bar{k})A_{k,\bar{k}} + \tilde{f}(-\bar{k},\bar{k})A_{k,-\bar{k}}\right] = A_{k,\bar{k}},\end{aligned} \tag{3.7}$$

where $\mathcal{P}$ denotes a principal value integration. One can check that the function $\mathcal{L}(\Omega_k)/(\bar{k}^2-k^2)$ is regular when $\bar{k} \to k$, and we used above that $\mathcal{L}(\Omega_{\bar{k}}) = 0$. Equation (3.7) is an inhomogeneous integral equation of the second kind for a given value of $\bar{k}$, which has a unique solution if the corresponding kernel is invertible. In principle, it may be solved numerically for any value of $\bar{k}$ to extract the value of a_{ad}.

However, the subsequent analysis is simplified considerably by letting $\bar{k} \to 0$. Formally, we expand Eq. (3.7) in $\bar{k}$ and keep only the lowest order. To that purpose, we first rewrite Eq. (3.7) in the form

$$\begin{aligned}&\frac{\mathcal{L}(\Omega_k)}{\bar{k}^2-k^2}2i\bar{k}\tilde{f}(k,\bar{k}) + i\mathcal{P}\int_{-\infty}^{\infty}\frac{dk'}{2\pi k'}\Big[\tilde{f}(k'+\bar{k},\bar{k})\,A_{k,k'+\bar{k}}\\ &-\tilde{f}(k'-\bar{k},\bar{k})\,A_{k,k'-\bar{k}}\Big]\\ &-\frac{1}{2}\left[\tilde{f}(\bar{k},\bar{k})A_{k,\bar{k}} + \tilde{f}(-\bar{k},\bar{k})A_{k,-\bar{k}}\right] = A_{k,\bar{k}}.\end{aligned}$$

Expanding in $\bar{k}$ and dividing by $2\bar{k}$, we then get to lowest order:

$$\begin{aligned}&-i\frac{\mathcal{L}(\Omega_k)}{k^2}\tilde{f}(k,0) + i\mathcal{P}\int_{-\infty}^{\infty}\frac{dk'}{2\pi k'}\partial_{k'}\left[A_{k,k'}\tilde{f}(k',0)\right]\\ &\qquad = A_{k,0}\left(\frac{\tilde{f}(0,\bar{k})+1}{2\bar{k}}\right)_{\bar{k}\to 0} + \frac{1}{2}\,\partial_{k'}A_{k,k'=0}.\end{aligned} \tag{3.8}$$

Finally, we integrate by parts, use Eqs. (3.2) and (3.6), and switch to dimensionless momenta by writing $k = 2\sqrt{\Omega_B}u$. Collecting terms, we then arrive at a tractable integral equation for $h(u) \equiv \tilde{f}(u,0)$. With the weakly Ω_B-dependent functions

$$G(u,u') = \sum_{p=0}^{\infty}\frac{4^{-p}}{1+u^2+u'^2+uu'+p/\Omega_B}, \tag{3.9}$$

$$H(u) = \sum_{p=0}^{\infty}\frac{4^{-p}u}{2(1+u^2+p/\Omega_B)^{-2}}, \tag{3.10}$$

this integral equation reads

$$\begin{aligned}&\int_{-\infty}^{\infty}\frac{du'}{2\pi u'^2}[G(u,u')h(u') - G(u,0)h(0)]\\ &-\frac{\sqrt{\Omega_B}}{2u^2}\mathcal{L}\left(\Omega_B\left[1+\frac{3u^2}{4}\right]\right)h(u)\\ &= \frac{a_{ad}\sqrt{\Omega_B}}{a_\perp}G(u,0) + iH(u).\end{aligned} \tag{3.11}$$

Note that the real (imaginary) part of $h(u)$ is even (odd) in u. The scattering length a_{ad} finally follows from the real part of Eq. (3.11) and the condition $h(0) = -1$, see Eq. (3.6), while b_{ad} can be extracted from the imaginary part of Eq. (3.11). The integral equation (3.11) shows in particular that $a_{ad}/a_\perp$ and $b_{ad}/a_\perp$ depend only on Ω_B, and hence only on the binding energy of the dimer. This already suggests universality of the three-fermion problem.

B. Dimer limit

The solution of this integral equation is discussed first for $a_\perp/a \gg 1$, where tightly bound dimers of size $a_B \approx a$ and large binding energy, $\Omega_B = (a_\perp/2a)^2 \gg 1$, are realized. Expanding the real part of Eq. (3.11) in $1/\Omega_B$, carefully including the Ω_B-dependence of $G(u,0)$ and $\mathcal{L}$, and using $\zeta(1/2, \Omega \gg 1) \approx -2\sqrt{\Omega}$, we obtain to first order

$$\begin{aligned}&\frac{3}{4}\frac{h(u)}{1+\sqrt{1+3u^2/4}} + \frac{3}{16}\frac{1}{\Omega_B}\frac{h_0(u)}{1+3u^2/4+\sqrt{1+3u^2/4}}\\ &+\frac{4}{3}\frac{1}{\Omega_B}\int_{-\infty}^{\infty}\frac{du'}{2\pi u'^2}\left(\frac{h_0(u')}{1+u^2+u'^2+uu'}+\frac{1}{1+u^2}\right)\\ &= \left(\frac{a_{ad}}{a_\perp\sqrt{\Omega_B}}\right)\left(\frac{4}{3}\frac{1}{1+u^2} - \frac{1}{\Omega_B}\frac{W_0}{(1+u^2)^2}\right)\end{aligned}$$

with $G(0,0) = 4/3$ and $W_0 = \sum_p p(1/4)^p = 4/9$. Here, we use the zeroth-order approximation $h_0(u)$ to the full solution $h(u)$. The lowest order gives

$$h_0(u) = -\frac{1}{2}\frac{1+\sqrt{1+3u^2/4}}{1+u^2}, \tag{3.12}$$

where $a_{ad} = -(9/32)\sqrt{\Omega_B}$ fixes $h_0(0) = -1$. The next order gives from $h(0) = -1$ a correction to the atom-dimer scattering length, such that

$$\begin{aligned} a_{ad} &= -\kappa_\infty a_\perp \sqrt{\Omega_B} + \beta a_\perp/\sqrt{\Omega_B} \\ &= -\kappa_\infty a_\perp^2/2a + 2\beta a, \end{aligned} \tag{3.13}$$

where $\kappa_\infty = 9/32 = 0.28125$ and

$$\beta = -\frac{9}{128} + \frac{3\sqrt{3}+4\pi}{8\pi} - \frac{3}{32} \simeq 0.5426. \tag{3.14}$$

Similarly, we can then compute $h(u)$ to first order in $1/\Omega_B$, and thereby obtain b_{ad} from the imaginary part of Eq. (3.11). Straightforward algebra gives

$$b_{ad}/a_\perp = (8/9)\Omega_B^{-3/2} \tag{3.15}$$

for $\Omega_B \gg 1$. The vanishing value of b_{ad} is a consequence of the short-rangedness of the effective atom-dimer potential [43]. The support of this potential is the dimer size $a_B \simeq a$ and goes to zero in the dimer limit. This validates a repulsive zero-range 1D atom-dimer potential in the low-energy limit, $V_{ad}(z) = g_{ad}\delta(z)$ with $g_{ad} \propto (-1/a_{ad})$, very similar to the 1D atom-atom scattering potential (1.8). In cold atom systems, the validity of our treatment in the dimer limit is always limited by the constraint that the 3D scattering length a is larger than the typical size of the actual atom-atom potential.

C. Numerical solution

Outside the dimer limit, in general a numerical solution of Eq. (3.11) is necessary. We describe next how an accurate numerical solution to Eq. (3.11) can be obtained in practice. One has to be quite careful to ensure regularity of $h(u)$, for which we found it beneficial to Fourier transform to real space, where the Fourier transformed h is well-behaved and allows for a quickly converging solution of the integral equation. In order to implement an efficient, fast and reliable numerical solution, it is mandatory to find a convenient representation of the integral kernel. As this is a nontrivial problem, we outline its solution in some detail here.

Let us first give some auxiliary relations that will be useful below. The function $\mathcal{L}$ appearing in Eq. (3.11) can be written as

$$\begin{aligned} \mathcal{L}(u) &= \zeta(1/2, \Omega_B(1+3u^2/4)) - \zeta(1/2,\Omega_B) \\ &= \frac{1}{\sqrt{\Omega_B}} \int_0^\infty \frac{dt}{\sqrt{\pi t}} \frac{e^{-t}}{1-e^{-t/\Omega_B}} \left(e^{-\frac{3}{4}u^2 t} - 1\right). \end{aligned}$$

In addition, $G(u,u')$ in Eq. (3.9) can alternatively be expressed in the form

$$G_{\Omega_B}(u,u') = \int_0^\infty \frac{dt}{1-\frac{1}{4}e^{-t/\Omega_B}} e^{-(1+u^2+uu'+u'^2)t}.$$

We then switch back to real space by writing

$$h(u) = -\int_{-\infty}^{\infty} dz e^{izu} g(z), \tag{3.16}$$

which leads to the Fourier transform of Eq. (3.11). The real part of this equation is

$$\int_{-\infty}^{\infty} dz' K(z,z') g(z') = -\frac{a_{ad}\sqrt{\Omega_B}}{a_\perp} B(z) \tag{3.17}$$

with

$$\begin{aligned} K(z,z') &= \int \frac{du}{2\pi} \int \frac{du'}{2\pi u'^2} e^{-izu} (G(u,u')e^{iz'u'} - G(u,0)) \\ &\quad - \frac{\sqrt{\Omega_B}}{2} \int \frac{du}{2\pi u^2} \mathcal{L}(u)\ e^{-i(z-z')u} \\ &= K_1(z,z') + K_2(z-z') \\ B(z) &= \int \frac{du}{2\pi} e^{-izu} G(u,0) = \sum_{p=0}^{\infty} 4^{-p} \frac{e^{-\sqrt{1+p/\Omega_B}|z|}}{2\sqrt{1+p/\Omega_B}}. \end{aligned} \tag{3.18}$$

Using the above auxiliary relations, some algebra gives with $X(t) \equiv |z'+z/2|/\sqrt{3t}$ and the probability function $\Phi(X)$ a convenient representation for the function K_1,

$$\begin{aligned} K_1(z,z') &= -\frac{\sqrt{3}}{4\sqrt{\pi}} \int_0^\infty dt \frac{e^{-t} e^{-z^2/4t}}{1-\frac{1}{4}e^{-t/\Omega_B}} \\ &\quad \times \left[X(t)\Phi(X(t)) + \frac{1}{\sqrt{\pi}} e^{-X^2(t)}\right]. \end{aligned} \tag{3.19}$$

In a similar fashion, with $Z(t) = |z-z'|/\sqrt{3t}$, we find

$$\begin{aligned} K_2(z-z') = \frac{1}{4}\sqrt{\frac{3}{\pi}} \int_0^\infty \frac{dt\, e^{-t}}{1-e^{-t/\Omega_B}} \\ \times \left(\frac{e^{-Z(t)^2}}{\sqrt{\pi}} + Z(t)[\Phi(Z(t)) - 1]\right). \end{aligned} \tag{3.20}$$

With $K(z,z') = K_1 + K_2$ and $B(z)$ given, one numerically computes $g(z)$ from Eq. (3.17) and then fixes a_{ad} from the normalization condition $\int dz g(z) = 1$ corresponding to $h(0) = -1$.

Let us first discuss this program in the BCS limit, $\Omega_B \ll 1$. Importantly, the kernel $K(z,z')$ is *not invertible* in this limit, since there is a zero mode solution $g_0(z)$. This function can be found analytically in momentum space using the Bethe Ansatz as described in Sec. VI B, with the result $h_0(u) = u/(1+u^2)$, leading to the real-space form $g_0(z) = \mathrm{sgn}(z) e^{-|z|}$. Fortunately, the zero mode does not affect the determination of the scattering length a_{ad}. To see this, note that $g_0(z)$ has odd parity and hence does not contribute to the normalization condition $\int dz\, g(z) = 1$. Since also the function $B(z)$ in Eq. (3.17) is even, we can restrict the numerical solution to even functions $g(z)$. On this space, $K(z,z')$ is invertible even in the BCS limit, and hence the numerical procedure is stable and reliable.

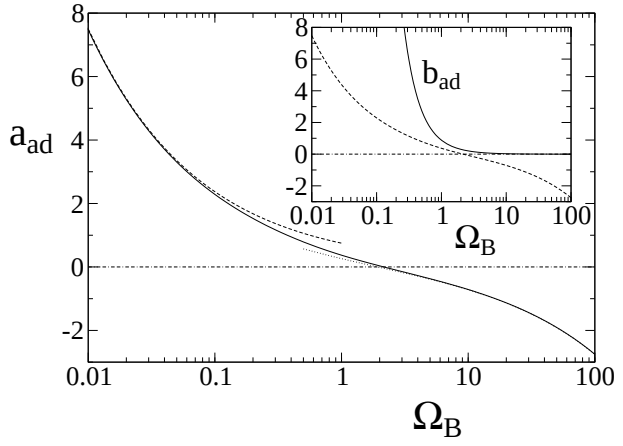


FIG. 1: Scattering length $a_{ad}/a_\perp$ versus dimensionless binding energy Ω_B. The solid curve is the numerical solution to Eq. (3.11), and the dotted (dashed) curves represent the analytical results in the dimer (BCS) limit, respectively. In the inset, $b_{ad}/a_\perp$ is plotted versus Ω_B. The solid curve gives b_{ad} from the numerical solution of Eq. (3.11), and the dashed line represents a_{ad} for comparison.

The numerical result for $a_{ad}/a_\perp$ as function of Ω_B, covering the full crossover, is shown in Figure 1. In the BCS limit, where $a_\perp/a \ll -1$ and $\Omega_B \ll 1$, the real part of Eq. (3.11) is solved by $h(u) = -1/(1+u^2)^2$, see Eq. (6.20) below, and hence we find the exact result

$$a_{ad} = \frac{3}{4}\, a_\perp/\sqrt{\Omega_B} = 0.75\, a_\perp^2/|a|. \qquad (3.21)$$

The numerical solution shown in Fig. 1 for arbitrary Ω_B nicely matches onto the analytically available limits (3.13) and (3.21). Remarkably, around $\Omega_B \approx 2.2$, there is a zero of the atom-dimer scattering length a_{ad}. One may suspect that this behavior is the analogue of the two-body CIR in Eq. (1.7). However, first one may notice that the atom-dimer 'resonance' occurs at a different Ω_B than the CIR. In addition, it is important to check whether one still has a simple contact δ-interaction potential, since otherwise the simple relationship $g_{ad} \propto -1/a_{ad}$ breaks down.

Let us then address the numerical evaluation of b_{ad} in Eq. (3.6), which is performed by looking at the imaginary part corresponding to Eq. (3.17),

$$\int_{-\infty}^{\infty} dz' K(z,z') g(z') = -B_2(z), \qquad (3.22)$$

where

$$\begin{aligned} B_2(z) &= \int \frac{du}{2\pi} e^{-izu}\, u\, H(u) \\ &= -i\,\frac{z}{8} \sum_{p=0}^{+\infty} \left(\frac{1}{4}\right)^p \frac{e^{-\sqrt{1+p/\Omega_B}|z|}}{\sqrt{1+p/\Omega_B}}. \end{aligned}$$

Once this integral equation is solved, b_{ad} follows as

$$\frac{b_{ad}}{a_\perp} = \frac{1}{2\sqrt{\Omega_B}} \int_{-\infty}^{\infty} dz\, z\, [-ig(z)]\,. \qquad (3.23)$$

Even though the kernel in Eq. (3.22) is the same as for the computation of a_{ad}, the situation is quite different in the BCS limit. The function $B_2(z)$ is an odd function of z and therefore not orthogonal to $g_0(z)$. This implies that the integral equation (3.22) has no solution when Ω_B is taken directly to zero. However, for any finite Ω_B, the kernel $K(z,z')$ becomes invertible, but the corresponding solution of (3.22) diverges for $\Omega_B \to 0$. The numerical result for b_{ad} is shown in the inset of Fig. 1. While in the dimer limit, b_{ad} stays small, in accordance with our analytical result (3.15), in the BCS limit, it is found to diverge as $b_{ad} \propto \Omega_B^{-3/2}$. We will see in Sec. VI that this divergence originates from the reflectionless scattering property encountered in the BCS limit. Moreover, these results for b_{ad} imply that one cannot use an effective δ-potential for the atom-dimer scattering outside the dimer limit. Notably, the vanishing of a_{ad} for $\Omega_B \simeq 2.2$ does not correspond to an atom-dimer resonance since $g_{ad} \propto (-1/a_{ad})$ breaks down away from the dimer limit.

IV. ROLE OF HIGHER TRANSVERSE CHANNELS

So far, the role of transverse excited states ($n \neq 0$) has been taken into account only through the exact calculation of $A_{k,k'}$ for $n = m = 0$. We still need to investigate the full Eq. (2.17) including higher transverse channels. In this section, we address their effect in detail. For the lowest channel $n = 0$, we keep using the Ansatz (3.4) for $f(k)$. For the higher channels, we have functions $f_n(k)$ instead. The full integral equation (2.17) [taking into account the rescaling discussed above] leads to a system of coupled integral equations for $f(k)$ and the $f_n(k)$. For the limit $\bar{k} \to 0$, following the line of reasoning in the last section, we arrive at the previous integral equation for $h(u)$ that now includes a coupling to the higher-channel modes

$$h_n(u) = \left[-if_n\left(k = 2\sqrt{\Omega_B}\, u\right)/\bar{k}\right]_{\bar{k}\to 0}.$$

The real and imaginary parts of $\{h(u), h_n(u)\}$ decouple in the resulting equations. For clarity, we show only the real part, which is sufficient to analyse the effect of the higher channels on the scattering length a_{ad}. After some algebra, we find

$$\begin{aligned} &\int_{-\infty}^{\infty} \frac{du'}{2\pi u'^2} [G^{0,0}(u,u')h(u') - G^{0,0}(u,0)h(0)] \qquad (4.1) \\ &-\frac{\sqrt{\Omega_B}}{2u^2}\mathcal{L}\left(\Omega_B[1+3u^2/4]\right) h(u) = \frac{a_{ad}\sqrt{\Omega_B}}{a_\perp} G^{0,0}(u,0) \\ &+\Omega_B \sum_{n'\neq 0} \int_{-\infty}^{\infty} \frac{du'}{\pi} G^{0,n'}(u,u') h_{n'}(u'), \end{aligned}$$

where the matrix elements $G^{n,n'}(u,u')$ can be extracted from the matrix elements $A^{n,n'}_{k,k'}$ defined in Eq. (2.20), with $G^{n,n'}(u,u') = \Omega_B A^{n,n'}_{k,k'}$ and the rescaling $k = 2\sqrt{\Omega_B}u$. We shall specify them in limiting cases below, but their general form for arbitrary parameters is of no interest here. Note that $G^{0,0}(u,u') = G(u,u')$ is given by Eq. (3.9). Furthermore, only modes with $m = m' = 0$ are coupled to the lowest transverse mode and thus have to be kept. Clearly, Eq. (3.11) is reproduced, but now includes a correction due to the higher channels. The integral equation is then closed by

$$\Omega_B^{-3/2}\int_{-\infty}^{\infty}\frac{du'}{2\pi u'^2}[G^{n,0}(u,u')h(u') - G^{n,0}(u,0)h(0)] + \mathcal{L}\left(n+\Omega_B[1+3u^2/4]\right)h_n(u) = \frac{a_{ad}}{a_\perp}\frac{G^{n,0}(u,0)}{\Omega_B} + \Omega_B^{-1/2}\sum_{n'\neq 0}\int_{-\infty}^{\infty}\frac{du'}{\pi}G^{n,n'}(u,u')h_{n'}(u'). \tag{4.2}$$

The system of integral equations given by Eqs. (4.1) and (4.2) will now be analyzed in the two limiting cases. In fact, we will see that in the BCS limit $a_\perp/a \to -\infty$, higher channels are completely negligible, while in the opposite dimer limit, they cause a renormalization of a_{ad} but no *qualitative* change in the picture put forward in the last section. Moreover, in the dimer limit, we can solve the problem analytically and establish a connection to the solution of the unconfined (3D) problem [35]. Since the effect of higher channels does not cause profound changes even in the dimer limit, we conclude that the physical picture of Sec. III is reliable and qualitatively correct for all $a_\perp/a$.

A. BCS limit

We now show that higher channels are indeed negligible in the BCS limit, $\Omega_B \ll 1$. As the channel index n has to be compared with the reduced energy Ω_B, it is intuitively clear that only small values of n can contribute. In addition, relevant wavevectors obey $k, k' \propto \sqrt{\Omega_B}$. To make this more quantitative, we specify $A^{n,n'}_{k,k'}$ in Eq. (2.20) for the BCS limit, which in turn determines $G^{n,n'}(u,u')$ appearing in Eqs. (4.1) and (4.2). For $\Omega_B \ll 1$, the integral representation

$$A^{n,n'}_{k,k'} \simeq \int_0^\infty dt e^{-\{\Omega_B+n'+[k'^2+k^2+kk']/4\}t} \times \int_0^\infty dx e^{-x}L_n(x)L_{n'}(x/4)$$

follows from Eq. (2.20). Both integrals can be directly computed, and we find $A^{n,n'}_{k,k'} = 0$ for $n > n'$ within these approximations, otherwise there are small corrections of order unity. For $n \le n'$, with an Ω_B-independent constant $C_{nn'}$, we obtain

$$A^{n,n'}_{k,k'} = \frac{C_{nn'}}{\Omega_B + (k^2+k'^2+kk')/4 + n'}.$$

Therefore, except for the open channel $n = n' = 0$, $A^{n,n'}_{k,k'}$ is always of order unity. Let us then analyze the scaling of the various terms in Eq. (4.2) as a function of $\Omega_B \ll 1$. On the left hand side, the first term scales as $\Omega_B^{-1/2}$, and the second as h_n. On the right hand side, the first term is at most of order $a_{ad}/a_\perp \propto \Omega_B^{-1/2}$, and the last term scales as $\Omega_B^{1/2}h_n$. Power counting then gives $h_n \propto \Omega_B^{-1/2}$. From Eq. (4.1), we now see that the last term (describing the effect of higher channels) scales as $\Omega_B^{3/2}$, and is thus negligible compared to the leading terms, which are of order unity. This fact allows us to safely conclude that higher transverse levels do not affect the low-energy scaling behavior of $a_{ad}/a_\perp$ in the BCS limit. This conclusion also holds for b_{ad} as one can show using a similar power counting reasoning.

B. Dimer limit

The situation is quite different in the dimer limit, $a_\perp/a \to +\infty$, where excited levels contribute to the asymptotic behavior of a_{ad} and b_{ad}. We first focus on the calculation of this correction for a_{ad}. In the dimer limit, relevant values for the channel number n are of order Ω_B, and we later introduce the rescaled continuous variable $p = 4n/3\Omega_B$ and convert the n-summation into an integration. Keeping only leading terms in $1/\Omega_B$, Eqs. (4.1) and (4.2) read

$$\frac{3}{4}\frac{h(u)}{1+\sqrt{1+3u^2/4}} = \frac{a_{ad}}{a_\perp\sqrt{\Omega_B}}G^{0,0}(u,0) + \frac{3}{2}\int_0^\infty dp'\int_{-\infty}^\infty\frac{du'}{2\pi}G^{0,p'}(u,u')\bar{h}_{p'}(u') \tag{4.3}$$

and

$$-2\left(\sqrt{1+3(u^2+p)/4}-1\right)\bar{h}_p(u) = \frac{a_{ad}}{a_\perp\sqrt{\Omega_B}}G^{p,0}(u,0) + \frac{3}{2}\int_0^\infty dp'\int_{-\infty}^\infty\frac{du'}{2\pi}G^{p,p'}(u,u')\bar{h}_{p'}(u'), \tag{4.4}$$

where we use $\bar{h}_p(u) = \Omega_B h_p(u)$. The second equation of this system is now independent of the first one and can be solved consistently. The kernel $G^{p,p'}(u,u')$ in the dimer limit $\Omega_B \gg 1$ follows from $A^{n,n'}_{k,k'}$, see Eq. (2.20), which has the integral representation

$$A^{n,n'}_{k,k'} = \int_0^\infty\frac{dt}{t}e^{-\{\Omega_B+n'+[k'^2+k^2+kk']/4\}\frac{3t}{4}} \times \int_0^\infty dx\, L_n(x)L_{n'}(x/4)e^{-x/t}. \tag{4.5}$$

To evaluate the x-integral, let us analyze the integral

$$\begin{aligned} I &= \int_0^\infty dx\, e^{-x/t}\, L_n(\lambda x) L_{n'}(\mu x) \\ &= t \int_0^\infty dy\, e^{-y}\, L_n(\lambda t y) L_{n'}(\mu t y). \end{aligned}$$

Now we define $\tilde{\lambda} = \lambda n t$ and $\tilde{\mu} = \mu n' t$, which stay constant in the limit $n, n' \to \infty$, and use an asymptotic property of the Laguerre polynomials, $\lim_{n\to\infty} L_n(x/n) = J_0(2\sqrt{x})$, where J_0 is a Bessel function. Therefore, the integral I in the limit of large n, n' is given by

$$\begin{aligned} I &= t \int_0^\infty dy e^{-y} J_0\left(2\sqrt{\tilde{\lambda} y}\right) J_0\left(2\sqrt{\tilde{\mu} y}\right) \\ &= 2t \int_0^\infty x dx e^{-x^2} J_0\left(2\sqrt{\tilde{\lambda}}\, x\right) J_0\left(2\sqrt{\tilde{\mu}}\, x\right). \\ &= t e^{-(\tilde{\lambda}+\tilde{\mu})} I_0\left(2\sqrt{\tilde{\lambda}\tilde{\mu}}\right). \end{aligned}$$

Setting $\lambda = 1$ and $\mu = 1/4$, using the integral representation for the Bessel function I_0,

$$I_0(x) = \int_0^{2\pi} \frac{d\varphi}{2\pi} e^{-x\cos\varphi},$$

and performing the t-integral in Eq. (4.5), we obtain

$$\begin{aligned} A^{n,n'}_{k,k'} &= \frac{4}{3} \int_0^{2\pi} \frac{d\varphi}{2\pi} \Big[\Omega_B + (k^2 + k'^2 + kk')/4 \\ &+ 4(n + n' + \sqrt{nn'}\cos\varphi)/3\Big]^{-1}. \end{aligned}$$

After rescaling $k = 2\sqrt{\Omega_B} u$ and $n = 3p/4\Omega_B$, we finally arrive at the expression

$$\begin{aligned} G^{p,p'}(u,u') &= \frac{4}{3} \int_0^{2\pi} \frac{d\varphi}{2\pi} \Big[1 + u^2 + u'^2 + uu' \\ &+ p + p' + \sqrt{pp'}\cos\varphi\Big]^{-1}. \end{aligned}$$

Inserting this result into Eq. (4.4), we can identify $(u, \sqrt{p}, \varphi)$ as the cylindrical coordinates of a 3D vector $\mathbf{r}$ (which is of course still a momentum operator), where $\bar{h}(\mathbf{r})$ is now a function of $\mathbf{r}$. Writing $h_o(\mathbf{r}) = r^2 \bar{h}(\mathbf{r})$, we obtain for the integral equation of the higher-channel modes (4.4) the form

$$\begin{aligned} &\frac{\sqrt{1 + 3r^2/4} - 1}{r^2}\, h_o(\mathbf{r}) + \int \frac{d\mathbf{r}'}{2\pi^2} \frac{h_o(\mathbf{r}')}{r'^2(1 + r^2 + r'^2 + \mathbf{r}\cdot\mathbf{r}')} \\ &= -\frac{2}{3}\left(\frac{a_{ad}}{a_\perp\sqrt{\Omega_B}}\right) \frac{1}{1 + r^2}. \end{aligned} \tag{4.6}$$

This integral equation is exactly the one governing the fermionic three-body problem without confinement [35]. The symmetry of Eq. (4.6) implies that $h_o(\mathbf{r})$ only depends on $r = |\mathbf{r}|$. We therefore write

$$h_o(\mathbf{r}) = -(2/3)\left(a_{ad}/a_\perp\sqrt{\Omega_B}\right) w_o(r), \tag{4.7}$$

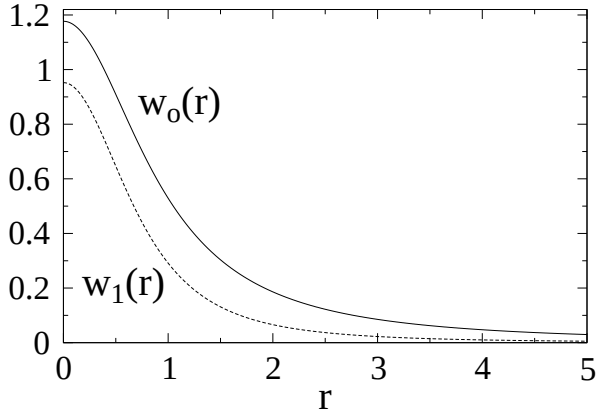


FIG. 2: Solutions $w_o(r)$ to Eq. (4.8), and $w_1(r)$ to Eq. (4.11).

where $w_o(r)$ is the solution to

$$\begin{aligned} &\frac{1}{\pi} \int_0^\infty \frac{dr'}{r\, r'} \ln\left(\frac{1 + r^2 + r'^2 + r\, r'}{1 + r^2 + r'^2 - r\, r'}\right) w_o(r') \\ &+ \frac{3}{4} \frac{w_o(r)}{1 + \sqrt{1 + 3r^2/4}} = \frac{1}{1 + r^2}. \end{aligned} \tag{4.8}$$

The numerical solution to this equation is shown in Fig. 2. We find $w_o(0) \simeq 1.179$, in accordance with STM's result $w_o(0) \approx 1.2$ [35, 36].

We now go back to Eq. (4.3) and consider $u = 0$. Straightforward algebra then gives to leading order in $1/\Omega_B$ the atom-dimer scattering length in the dimer limit as

$$-\frac{a_{ad}}{a_\perp\sqrt{\Omega_B}} \equiv \kappa_\infty = \frac{3}{4 w_o(0)} \simeq 0.636. \tag{4.9}$$

This value should be compared to $\kappa_\infty = 9/32 = 0.28125$, which results when higher channels are neglected, see Eq. (3.13). Note that our result makes explicit contact to the previous solution for the unconfined case [35, 36]. This is also seen by writing Eq. (4.9) as

$$a_{ad} = -\frac{a^2_{red,\perp}}{2(w_o(0)\, a)} \tag{4.10}$$

with the confinement scale $a_{red,\perp} = (3\hbar/2m_0\omega_\perp)^{1/2}$ for reduced mass $2m_0/3$ of the atom-dimer complex. With the 3D atom-dimer scattering length $w_o(0)a = w_o(0)/\kappa_B$, this result exactly matches the dimer limit of the analogous two-body result (1.7). Equation (4.10) predicts that the product of the 1D and 3D atom-dimer scattering lengths (in units of $a_\perp$) is a universal constant, independent of the atomic properties. In fact, we shall see later that it is even independent of statistics.

Let us then turn to the determination of b_{ad} in the dimer limit, including the contribution of higher transverse channels. The calculation follows closely the one for a_{ad}, and we shall therefore only briefly outline the

various steps. Starting with the imaginary part of the general coupled equations resulting from (2.17), we arrive at new coupled equations very similar to Eqs. (4.1) and (4.2). We then use the asymptotic expression for $A^{n,n'}_{k,k'}$ in the dimer limit and perform the rescaling $k = 2\sqrt{\Omega_B}u$, $n = 3p/4\Omega_B$ and $\bar{h}_p(u) = \Omega_B h_p(u)$. Once again we identify $(u, \sqrt{p}, \varphi)$ as the cylindrical coordinates of a 3D vector $\mathbf{r}$, and, in order to obtain an integral equation with a spherically symmetric solution, we define $\mathrm{Im}\,\bar{h}(\mathbf{r}) = -(u/r^2)\,(1/\Omega_B)\,w_1(r)$. After some algebra, we eventually obtain an integral equation for $w_1(r)$ very similar to Eq. (4.8), namely

$$\frac{3}{4}\frac{w_1(r)}{1+\sqrt{1+3r^2/4}}+\frac{1}{\pi}\int_0^\infty dr' K(r,r')w_1(r') = \frac{1}{3(1+r^2)^2}, \tag{4.11}$$

with the kernel

$$K(r,r') = \frac{1}{r^2}\left(2-\frac{1+r^2+r'^2}{rr'}\ln\left(\frac{1+r^2+r'^2+rr'}{1+r^2+r'^2-rr'}\right)\right). \tag{4.12}$$

The numerical solution to this equation is shown in Fig. 2. Including the higher channels, we thus find for b_{ad} instead of Eq. (3.15) the result

$$\frac{b_{ad}}{a_\perp} = \frac{w_1(0)}{\Omega_B^{3/2}}, \quad w_1(0) \simeq 0.952. \tag{4.13}$$

Notably, this is essentially the same behavior as in Eq. (3.15), where the higher channels were neglected. Even the coefficient of the asymptotic behavior, 0.952 compared to $8/9 \simeq 0.889$, is very close.

To summarize, we conclude that in the deep dimer limit, the relevant physics is not changed by the confinement potential.

V. BOSONIC THREE-BODY PROBLEM

In this section, we consider the problem of three identical bosons in a tight transverse harmonic confinement, allowing to analyze the 1D bosonic analogue of the problem studied up to now for fermions. The main difference is that the three-body wavefunction is now totally symmetric. On a formal level, the calculation is similar to the fermionic one, so in what follows we go through it, highlighting the differences and keeping the same notation as much as possible. The definition of the coordinate system remains the same, i.e., $\mathbf{x_1}$, $\mathbf{x_2}$ and $\mathbf{x_3}$ are the 3D positions of the bosons. Next the orthogonal transformation (2.1) to variables $(\mathbf{x}, \mathbf{y}, \mathbf{z})$ is performed. The harmonic trap potential is still diagonal in the positions after this transformation, and the center-of-mass coordinate $\mathbf{z}$ again decouples. Hence the three-body problem reduces to

$$\left(-\frac{\hbar^2}{m_0}\nabla^2_{\mathbf{X}} + U_c(\mathbf{X}) - E\right)\Psi(\mathbf{X}) = -\left[V(\mathbf{y}) + \sum_{\pm} V(\mathbf{r}_\pm)\right]\Psi(\mathbf{X}). \tag{5.1}$$

As in Eq. (2.3), $\mathbf{r}_\pm$ denotes the distance between the boson at $\mathbf{x_1}$ and the $\mathbf{x_2}$ or $\mathbf{x_3}$ particles, respectively, while $\mathbf{y} = \mathbf{x_2} - \mathbf{x_3}$. Note that all three bosons interact, leading to the extra term $V(\mathbf{y})$ in Eq. (5.1) compared to the fermionic Eq. (2.2). Incorporating atom-atom interactions via the pseudopotential approach, one boundary condition now reads

$$\Psi(\mathbf{X}) \simeq \frac{f(\mathbf{x})}{4\pi}\left[\frac{1}{y}-\frac{1}{a}\right], \quad \mathbf{y}\to 0, \tag{5.2}$$

while the other two are

$$\Psi(\mathbf{X}) \simeq \frac{f(\mathbf{r}_{\perp,\pm})}{4\pi}\left[\frac{1}{r_\pm}-\frac{1}{a}\right], \quad \mathbf{r}_\pm \to 0, \tag{5.3}$$

where $\mathbf{r}_{\perp,\pm} = -\cos(\theta)\mathbf{x} \pm \sin(\theta)\mathbf{y}$ carries an extra minus sign compared to Eq. (2.11). Because the three-body wavefunction is fully symmetric, the conditions (5.3) are redundant, and it is sufficient to satisfy only Eq. (5.2) in what follows. As discussed in the Introduction, the bosonic three-body problem requires a short-distance regularization R^*, which we implement using Petrov's scheme [41]. The regularization (1.9) is formulated via the action of a differential operator on the scattering amplitude that describes the relative kinetic and confinement energy. The boundary condition (5.2) (for $\mathbf{y}\to 0$) is thereby modified to

$$\Psi(\mathbf{X}) \simeq \left[\frac{1}{y}-\frac{1}{a}-R^*\left(\frac{m_0 E}{\hbar^2}+\nabla^2_{\mathbf{x}}-\frac{2\rho^2_{\mathbf{x}}}{a^4_\perp}\right)\right]\frac{f(\mathbf{x})}{4\pi}, \tag{5.4}$$

where $\rho_{\mathbf{x}}$ is the component of $\mathbf{x}$ along the transverse direction. The boundary condition for the two-body problem also changes, now leading to a modified equation for the dimensionless binding energy Ω_B defined in Eq. (1.4). Instead of Eq. (1.5), it now reads

$$\zeta(1/2,\Omega_B) + a_\perp/a - 4R^*\Omega_B/a_\perp = 0. \tag{5.5}$$

In the dimer limit, $\Omega_B \gg 1$, the 3D result [41] follows,

$$\kappa_B = \frac{1}{2R^*}\left(\sqrt{1+\frac{4R^*}{a}}-1\right), \tag{5.6}$$

while in the BCS limit, R^* gives only subleading corrections.

In an identical way as for fermions, we then obtain the bosonic analogue of Eq. (2.13), take the $\mathbf{y}\to 0$ limit according to Eq. (5.4), and finally obtain the integral equation like in Eq. (2.17). This modified integral equation for bosons reads

$$\widetilde{\mathcal{L}}(\Omega_\lambda) f_\lambda = \sum_{\lambda'} \widetilde{A}_{\lambda,\lambda'} f_{\lambda'}, \tag{5.7}$$

where Ω_λ is given by Eq. (2.19), and the matrix elements are

$$\widetilde{A}_{\lambda,\lambda'} = -\frac{8\pi\hbar^2\, a_\perp}{m_0}\int d\mathbf{x}\,\psi^*_\lambda(\mathbf{x})\,\psi_{\lambda'}(-\mathbf{x}\cos\theta)\times \times G_{E-E'_\lambda}(\mathbf{x}\sin\theta,0). \tag{5.8}$$

When compared to the fermionic Eq. (2.20), the bosonic Eq. (5.8) carries an overall factor of -2, implying that an effective repulsion has turned into an attractive force. Moreover, the integrand in Eq. (5.8) remains unaltered since $\cos 2\theta = -\cos\theta$ and $\sin 2\theta = \sin\theta$. In addition, the $\mathcal{L}$ function (2.18) is modified to

$$\widetilde{\mathcal{L}}(\Omega_\lambda) = \zeta(1/2,\Omega_\lambda) - \zeta(1/2,\Omega_B) - R^*(k^2-\bar{k}^2+2n), \tag{5.9}$$

where from now on, all lengths (momenta) will again be given in units of $a_\perp$ ($1/a_\perp$). Note that the distance between the center-of-mass of the two bosons $\mathbf{x_{2,3}}$ and the one at $\mathbf{x_1}$ is $\mathbf{x}\sin\theta$. Since $\sin\theta = \sin(2\theta)$, exactly the same rescaling as in the fermionic case will be employed in what follows.

A. Scattering solution

Let us then proceed by projecting Eq. (5.7) onto the ground state. We use the same scattering Ansatz (3.4) as for fermions, and after expanding in $\bar{k} = 2\sqrt{\Omega_B}\,\bar{u}$, one easily obtains the bosonic version of Eq. (3.11),

$$\int_{-\infty}^{\infty}\frac{du'}{2\pi u'^2}[G(u,u')h(u') - G(u,0)h(0)] + \frac{\sqrt{\Omega_B}}{4u^2}\widetilde{\mathcal{L}}(u)h(u) = \frac{a_{ad}\sqrt{\Omega_B}}{a_\perp}G(u,0) + iH(u), \tag{5.10}$$

with the functions $G(u,u')$ and $H(u)$ defined as for fermions, see Eqs. (3.9) and (3.10). Furthermore, Eq. (5.9) gives

$$\begin{aligned}\widetilde{\mathcal{L}}(u) &= \zeta\left(1/2,\Omega_B(1+3u^2/4)\right) \\ &- \zeta(1/2,\Omega_B) - 3R^*\Omega_B u^2.\end{aligned} \tag{5.11}$$

In the bosonic case, the atom-dimer scattering length $a_{ad}/a_\perp$ therefore depends on the two dimensionless parameters Ω_B and $R^*/a_\perp$. In that sense, the bosonic problem is non-universal [19].

Let us start with the *dimer limit*, $\Omega_B \gg 1$. In that case it is useful to introduce the dimensionless regularization parameter

$$r^* = \kappa_B R^* = \frac{1}{2}\left(\sqrt{1+\frac{4R^*}{a}}-1\right). \tag{5.12}$$

The solution to Eq. (5.10) in the dimer limit can be found analytically again, with the result

$$\frac{a_{ad}}{a_\perp} = \frac{9}{64(1+2r^*)}\sqrt{\Omega_B} + \frac{\beta}{\sqrt{\Omega_B}}, \tag{5.13}$$

where the coefficient β is given for $r^*=0$ as

$$\beta = 9/256 + (3\sqrt{3}+4\pi)/8\pi + 3/64 \simeq 0.6638.$$

We also find $b_{ad}/a_\perp = -(4/9)\Omega_B^{-3/2}$, which resembles the fermionic equivalent (3.15).

However, as in the fermionic case, Eq. (5.10) is not sufficient in the dimer limit, and higher transverse channels must be included. Skipping details of the calculation – which closely parallels the fermionic one in Sec. IV B – and keeping the same notation, we find instead of Eq. (4.6) the bosonic scattering solution

$$\begin{aligned}&\frac{\sqrt{1+3r^2/4}-1+3r^*r^2/4}{r^2}\,h_o(\mathbf{r}) \\ &-\int\frac{d\mathbf{r}'}{\pi^2}\frac{h_o(\mathbf{r}')}{r'^2(1+r^2+r'^2+\mathbf{r}\cdot\mathbf{r}')} = \\ &+\frac{4}{3}\left(\frac{a_{ad}}{a_\perp\sqrt{\Omega_B}}\right)\frac{1}{1+r^2}.\end{aligned} \tag{5.14}$$

Defining the function $w_o(r)$ as in Eq. (4.7), we obtain after angle integration instead of Eq. (4.8) the equation

$$\begin{aligned}&\frac{\sqrt{1+3r^2/4}-1+3r^*r^2/4}{2r^2}\,w_o(r) = -\frac{1}{1+r^2} \\ &+\ \frac{1}{\pi}\int_0^\infty\frac{dr'}{r\,r'}\ln\left(\frac{1+r^2+r'^2+r\,r'}{1+r^2+r'^2-r\,r'}\right)w_o(r').\end{aligned} \tag{5.15}$$

At $r^*=0$, this is precisely STM's Eq. (15) [35], once the 3D scattering length is identified with $w_o(0)a_B = w_o(0)/\kappa_B$. For finite r^*, it is equivalent to the equation recently studied by Petrov, since Eq. (5.15) follows from Eq. (12) of Ref. [41] upon substitution of the standard 3D scattering Ansatz. The scattering length can be extracted in a way similar to the fermionic case. For that purpose, we put $u=0$ in the bosonic version of Eq. (4.3), and arrive at

$$-\frac{3}{8}(1+2r^*) = -\frac{8}{3}\frac{a_{ad}}{a_\perp\sqrt{\Omega_B}}\left[1-\frac{2}{\pi}\int_0^\infty dr\frac{w_o(r)}{1+r^2}\right].$$

On the other hand, taking $r\to 0$ in Eq. (5.15) yields

$$\frac{3}{8}(1+2r^*)\frac{w_o(0)}{2} = -1+\frac{2}{\pi}\int_0^\infty dr\frac{w_o(r)}{1+r^2}.$$

Consequently we have

$$\frac{a_{ad}}{a_\perp\sqrt{\Omega_B}} = -\frac{3}{4w_o(0)}, \tag{5.16}$$

i.e., the same relation as for fermions, leading to Eq. (4.10) and matching the analogous two-body result (1.7). We conclude that in the dimer limit, for both fermions and bosons, the 1D scattering length a_{ad} is always inversely proportional to the 3D scattering length $w_o(0)/\kappa_B$. The latter has been studied in detail in Ref. [41] as a function of R^*/a. It was found to diverge whenever a new Efimov state splits from the continuum,

going through zero in between the resonances, see Fig. 1 of Ref. [41]. According to Eq. (5.16), the atom-dimer scattering length a_{ad} will behave in the opposite manner, i.e., it vanishes every time a new bound state emerges and diverges in between. Note that in order to derive Eq. (5.14), one needs to impose $w_o(0)/\kappa_B < a_\perp$, which follows from $\Omega_B \gg 1$, so that divergences of $w_o(0)/\kappa_B$ will in practice be smeared out on lengthscales $\approx a_\perp \gg a$.

In the limit of large R^*, one can solve Eq. (5.15) analytically by expanding in inverse powers of r^* [41],

$$w_o(r) = -\frac{8}{3r^*}\frac{1}{1+r^2} + \mathcal{O}(1/r^{*2}).$$

Taking into account Eqs. (5.6) and (5.12), it is easily seen that the 3D scattering length becomes independent of R^*, while for the 1D scattering length, the contribution of higher channels clearly becomes negligible. We then obtain from Eq. (5.13)

$$a_{ad} = \frac{9}{64}\frac{a_\perp^2}{a}, \tag{5.17}$$

which is a universal result in the sense that it does not depend on R^*.

Higher channels can also be taken into account exactly for the calculation of b_{ad} in the dimer limit. We follow the fermionic case in Sec. IV B and obtain

$$\frac{b_{ad}}{a_\perp} = -\frac{w_1(0)}{\Omega_B^{3/2}}, \tag{5.18}$$

where, in contrast to the fermionic case, $w_1(r)$ solves the integral equation

$$\begin{aligned}&\frac{3}{4}\frac{w_1(r)}{1+\sqrt{1+3r^2/4}} + \frac{3}{8}r^* w_1(r)\\ &\quad - \int_0^\infty \frac{dr'}{\pi} K(r,r') w_1(r') = \frac{1}{3(1+r^2)^2},\end{aligned} \tag{5.19}$$

with $K(r,r')$ given by Eq. (4.12). The solution for $w_1(0)$ as a function of R^*/a is shown in Fig. 3. Apparently, there is no divergence due to Efimov states. In particular, the $R^* \to 0$ limit is well-defined, with $w_1(0) \simeq 1.59$, and

$$b_{ad} \simeq -12.7 a^3/a_\perp^2, \tag{5.20}$$

validating a zero-range atom-dimer potential in the low-energy limit. The other limit is $R^* \gg a$, where $w_1(0) \simeq (8/9)\sqrt{a/R^*}$, and therefore

$$b_{ad} = -(64/9) R^* (a/a_\perp)^2. \tag{5.21}$$

Comparing this result to Eq. (5.17), we find that the zero-range potential approximation requires $R^* a^3/a_\perp^4 \ll 1$, which self-consistently holds for $\Omega_B \gg 1$.

In the BCS limit, $\Omega_B \ll 1$, the same argument as in Sec. IV A can be applied to the bosonic case. Therefore higher channels can again be disregarded in that limit.

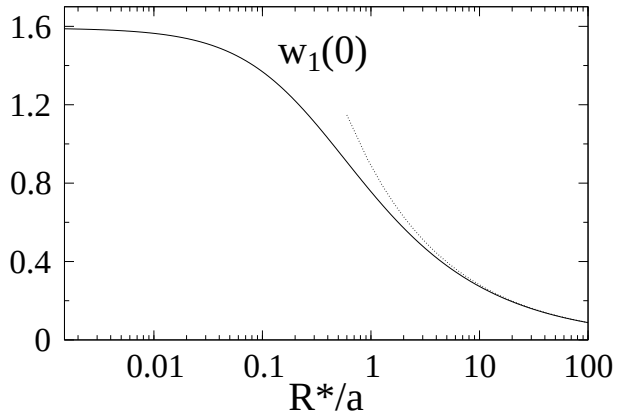


FIG. 3: Solution $w_1(0)$ (full line) to Eq. (5.19) as a function of R^*/a. The dotted curve gives the asymptotic behavior $w_1(0) = (8/9)\sqrt{a/R^*}$ for large R^*/a.

Moreover, the regularization parameter R^* drops out to leading order, since relevant momenta are small ($\propto \sqrt{\Omega_B}$) and the short-ranged cutoff ceases to matter. In this sense, the three-body problem becomes universal again in the BCS limit. The asymptotic behavior of a_{ad} and b_{ad} can be analytically computed using the Bethe Ansatz, see Sec. VI. One can verify that $h(u) = -2u/(1+u^2)^2$ solves the imaginary part of Eq. (5.10) in the BCS limit, leading to

$$\frac{b_{ad}}{a_\perp} = \frac{h'(0)}{2\sqrt{\Omega_B}} = -\frac{1}{\sqrt{\Omega_B}}. \tag{5.22}$$

For the real part of Eq. (5.10), we obtain from the Bethe Ansatz the solution

$$h(u) = 4\,\frac{a_{ad}\sqrt{\Omega_B}}{a_\perp}\,\frac{u^2}{1+u^2} \tag{5.23}$$

in the BCS limit. Evidently, the condition $h(0) = -1$ cannot be fulfilled for any finite a_{ad}. Similarly to b_{ad} for the fermionic case, the asymptotic behavior of a_{ad} is therefore expected to diverge as $a_{ad} \propto -1/\Omega_B^{3/2}$ when approaching the BCS limit. We shall discuss this point in detail in Sec. VI.

For the general case of arbitrary $a_\perp/a$, we have solved numerically the real-space version of Eq. (5.10) as in Sec. III C, neglecting higher channels. For the sake of simplicity, we take $R^* = 0$. When compared to the fermionic Eq. (3.17), the kernel (3.18) is now $K = K_1 - K_2/2$, with $K_{1,2}$ given in Eqs. (3.19) and (3.20), respectively. The results are shown in Fig. 4. Clearly, they closely match the predicted behavior in both limits. A finite R^* in Eq. (3.17) gives similar results. From the above discussion, this is clear in the BCS limit. Moreover, when just keeping the lowest transverse channel, the qualitative behavior is not modified in the dimer limit either. Therefore we expect a very similar picture for arbitrary R^* as the one shown for $R^* = 0$ in Fig. 4, as

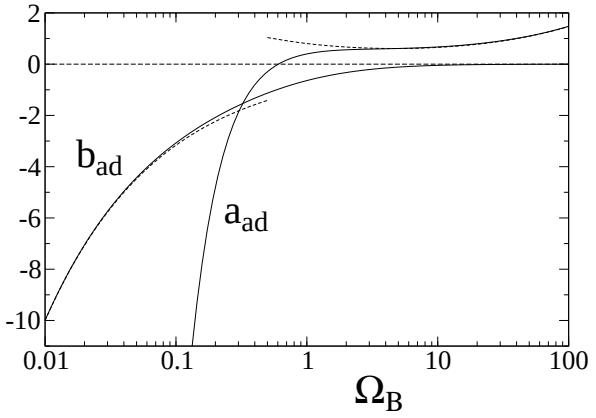


FIG. 4: Plot of a_{ad} and b_{ad} (full lines) as function of the dimensionless binding energy Ω_B for the three-boson problem at $R^* = 0$. The asymptotic behavior is shown (i) for b_{ad} in the BCS limit, $-1/\sqrt{\Omega_B}$, and (ii) for a_{ad} in the dimer limit, $(9/64)\sqrt{\Omega_B} + 0.6638/\sqrt{\Omega_B}$.

long as higher channels can be neglected [as presumed in Eq. (3.17)]. While this approximation is justified in the BCS limit, in the dimer limit it does not capture the correct asymptotic behavior, except for large R^*/a, see above. In particular, the influence of Efimov states on a_{ad} becomes important and affects the physics in the dimer limit in a significant way. This is in contrast to the fermionic case, where the projection onto the lowest transverse state already yields the qualitatively correct behavior even in the dimer limit.

B. Bound States: Trimers

For the bosonic problem, one expects atom-dimer bound states (trimers) to form under certain conditions. We therefore next derive the relevant integral equation. In this case, the scattering Ansatz cannot be used, and the resulting homogeneous integral equation must be considered. The total energy of the system is now $E = -2\,\hbar\omega_\perp\Omega_B - E_T$, where the trimer binding energy is written as

$$E_T = \frac{3}{4}\frac{\hbar^2}{m_0}\kappa_B^2 u_0^2, \tag{5.24}$$

with u_0 being the inverse size of the trimer in units of $a_B = 1/\kappa_B$. Projecting Eq. (5.7) onto the transverse ground state, we find

$$\begin{aligned}&\left[\zeta\left(\frac{1}{2}, \Omega_B(1+\frac{3}{4}(u^2+u_0^2)\right) - \zeta\left(\frac{1}{2}, \Omega_B\right)\right.\\ &-\left. 3\Omega_B R^*(u^2+u_0^2)\right] f(u)\\ &= -\frac{2}{\pi\sqrt{\Omega_B}}\int_{-\infty}^{\infty} du' G_{u_0}(u,u') f(u'),\end{aligned} \tag{5.25}$$

where the function $G_{u_0}(u,u')$ is defined by

$$G_{u_0}(u,u') = \sum_{p=0}^{\infty} \frac{4^{-p}}{1+3u_0^2/4+u^2+u'^2+uu'+p/\Omega_B}.$$

Equation (5.25) is then an eigenvalue equation for u_0.

First, we study Eq. (5.25) in the dimer limit. In order to obtain a nontrivial solution, we need to consider $u_0 \ll 1$. Then $f(u)$ is dominated by its small-u behavior, and using Eq. (5.12), Eq. (5.25) is simplified to give

$$f(u) = \frac{1}{u_0^2+u^2}\frac{32}{9\pi\Omega_B(1+2r^*)}\int_{-\infty}^{\infty} du' f(u'), \tag{5.26}$$

which implies $f(u) \propto 1/(u^2+u_0^2)$. Self-consistency of this expression leads to

$$u_0 = \frac{32}{9\Omega_B(1+2r^*)}\,. \tag{5.27}$$

Note that we have supposed here that $f(u)$ is an even function. Taking instead an odd function, we get

$$f(u) = \frac{u}{u_0^2+u^2}\,\frac{32}{9}\frac{1}{\pi\Omega_B(1+2r^*)}\int_{-\infty}^{\infty} du' u' f(u'),$$

which does not allow for a non-trivial and self-consistent solution. Therefore $f(u)$ cannot be odd in the dimer limit. For large r^*, the trimer binding energy becomes universal, and is given by

$$E_T = \frac{1024}{27}\frac{\hbar^2}{m_0}\frac{a^2}{a_\perp^4}. \tag{5.28}$$

Note that the existence of this novel *confinement-induced trimer state* (CIT) is consistent with the positive 1D atom-dimer scattering length for bosons found in the dimer limit, see Eq. (5.17).

In the BCS limit, Eq. (5.25) for the bound states reduces to

$$\begin{aligned}&\left[\frac{1}{\sqrt{1+3(u^2+u_0^2)/4}} - 1\right] f(u)\\ &= -\frac{2}{\pi}\int_{-\infty}^{\infty}\frac{du' f(u')}{1+3u_0^2/4+u^2+u'^2+uu'}\,.\end{aligned} \tag{5.29}$$

The fact that one can use the Bethe Ansatz to solve directly the BCS limit also holds for bound states. Indeed, we will verify in Sec. VI that Eq. (5.29) follows from a 1D Schrödinger equation, see Eq. (6.4) below, and leads to the exact solution

$$f(u) = \frac{1}{u^2+u_0^2} \tag{5.30}$$

for $u_0 = 2$. We have verified numerically that there are no other solutions, neither even nor odd. In fact, in real space, Eq. (5.30) is nothing but the known bound-state

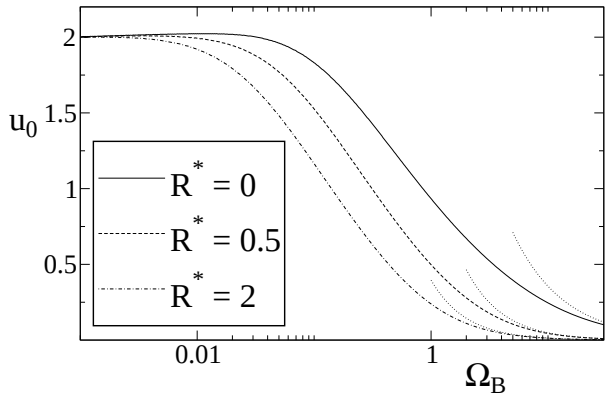


FIG. 5: Parameter u_0 appearing in the trimer binding energy, Eq. (5.24), as a function of Ω_B for various values of $R^*/a_\perp$. The dotted lines correspond to the asymptotic behavior in the dimer limit, Eq. (5.27).

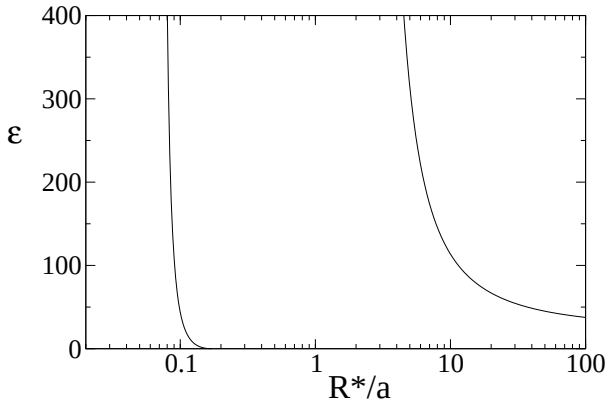


FIG. 6: Reduced energy $\epsilon \equiv (E_T/\hbar\omega_\perp)(a_\perp/a)^2$ for the CIT in the dimer limit as a function of R^*/a.

Bethe function for three attractively interacting bosons [29],

$$\psi \propto \exp\left[-(|z_1 - z_2| + |z_2 - z_3| + |z_3 - z_1|)/a_{aa}\right]. \tag{5.31}$$

In between the BCS and the dimer limits, we have investigated Eq. (5.25) numerically, see Fig. 5. Qualitatively, we see that the trimer energy barely depends on R^*, and in the BCS limit even becomes completely independent of this regularization parameter. However, Eq. (5.25) is only approximate since it is derived by projecting Eq. (5.7) onto the lowest transverse state, and therefore does not include the effect of higher channels. Notably, Efimov trimer states cannot be recovered within this approximation. Such states are irrelevant in the BCS limit, where the lengthscale a_{aa} of the confined trimer state [see Eq. (5.31)] is larger than the typical lengthscale a of Efimov states, so that the two problems decouple. However, when moving towards the dimer limit, the interplay between the confined trimer state and Efimov states plays a role.

In the dimer limit, it is possible to study the CIT in a quantitative manner, including the way it is affected by Efimov trimer states. In fact, we have shown in Sec. V A, for the dimer limit, that the low-energy atom-dimer scattering properties are described by a 1D contact potential $V(z) = (-2\hbar^2/m_0 a_{ad})\delta(z)$. This potential has a bound state for $a_{ad} > 0$ and its energy is given by

$$E_T = \frac{\hbar^2}{m_0\, a_{ad}^2}. \tag{5.32}$$

The corresponding 1D scattering length a_{ad} is related through Eq. (4.10) to the 3D atom-dimer scattering length $w_o(0)a_B$ (i.e., without external confinement) obtained from the solution of Eq. (5.15). This quantity is shown, e.g., in Fig. 1 of Ref. [41]. The bound state of this 1D contact potential – present only for $a_{ad} > 0$ – describes the CIT as long as its energy $E_T < \hbar\omega_\perp$. This implies $a_{ad} > a_\perp$, which in turn is equivalent to the condition $w_o(0)a_B < a_\perp$. This coincides with the condition in Sec. V A for the validity of Eq. (5.14), and therefore of Eq. (4.10) for bosons. The CIT is thus present only for $w_o(0)a_B < 0$, and its energy follows from Eqs. (5.32) and (4.10) in the form

$$\frac{E_T}{\hbar\omega_\perp} = \left(\frac{a}{a_\perp}\right)^2 \frac{32}{9} \left(\frac{w_o(0)\, a_B}{a}\right)^2. \tag{5.33}$$

From the numerical solution of Eq. (5.15), we obtain results for E_T as a function of R^*/a, see Fig. 6. Obviously, in the dimer limit, the CIT only exists for certain values of R^*/a. While it is present for all values larger than $R^*/a \simeq 2.2$, below this threshold, it disappears and reappears periodically for decreasing R^*/a. One such cycle is shown in Fig. 6, where the CIT has disappeared in the window $0.17 \lesssim R^*/a \lesssim 2.2$, but reappears for $R^*/a \lesssim 0.17$. For $R^* \ll a$, the behaviour is exactly periodic as a function of $\ln(R^*/a)$ and can be obtained analytically using the known result [19]

$$\frac{w_o(0)a_B}{a} = 1.46 - 2.15 \tan\left[1.00624 \ln(a\Lambda^*) + 0.09\right], \tag{5.34}$$

together with $\Lambda^* \simeq 6.6/R^*$ [41]. The ultimate fate of the CIT and its evolution in between the BCS and the dimer limits remains a difficult open question that is outside the scope of our paper.

VI. BETHE ANSATZ IN THE BCS LIMIT

In the BCS limit, $\Omega_B \to 0$, the role of transverse excited states is negligible. Confined in the transverse ground state, the motion of particles becomes effectively 1D, with contact δ-interactions between bosons or between distinguishable fermions. This strong simplification of the original 3D hamiltonian hence allows for exact solutions on the many-body level, namely the Lieb-Liniger model for bosons [44], or the Yang-Gaudin model

for fermions [45], both based on the powerful Bethe Ansatz. Recently, these two models have been used to study many-body properties of cold atoms in 1D confined geometries [20, 21]. In this section, we use the Bethe Ansatz [29] to solve the three-body problem for bosons and fermions in the BCS limit. This leads to analytical predictions for a_{ad} and b_{ad}, as well as for the bosonic trimer state. We thereby derive some of the results presented in previous sections. Noting that the atom-dimer scattering does not lead to any reflected wave, we also clarify the connection between the divergence of a_{ad} (b_{ad}) for bosons (fermions) and the fact that the scattering process is reflectionless. The reduction of the original problem to a 1D model is not completely straightforward and needs to be considered cautiously. Even in the BCS limit, the few-body wavefunction is not restricted to the transverse ground state. In order to build up a boundary condition like Eq. (2.4), imposed by the two-body potential for small particle distances, many excited transverse states have to be involved. However, as soon as distances between particles are larger than $a_\perp$, essentially only the transverse ground state can be occupied. In our case, the relevant lengthscale is the 1D scattering length $a_{aa} = a_\perp^2/2|a| \gg a_\perp$, which justifies the neglect of transverse excited states. This simplification becomes incorrect for problems involving lengthscales $\leq a$, e.g., when describing deeply bound Efimov states or three-body recombination processes.

Let us first explicit the connection between our integral equations in the BCS limit and the 1D reduced problem. We start with bosons. The 1D Schrödinger equation is

$$\left[-(\partial_{z_1}^2+\partial_{z_2}^2+\partial_{z_3}^2)-\frac{2m_0E}{\hbar^2}\right]\psi(z_1,z_2,z_3)= \\ \frac{4}{a_{aa}}\left[\delta(z_1-z_2)+\delta(z_1-z_3)+\delta(z_2-z_3)\right]\psi(z_1,z_2,z_3), \tag{6.1}$$

where the two-body 1D contact interaction can be recovered by projecting the 3D pseudopotential to the lowest transverse state,

$$-\frac{2\hbar^2}{m_0 a_{aa}}\delta(z)=\int \rho d\rho d\phi\; R_{00}(\rho)\frac{4\pi\hbar^2 a}{m_0}\delta(\mathbf{r})\frac{\partial}{\partial r}(r\cdot)R_{00}(\rho). \tag{6.2}$$

We then closely follow Sec. II, with the 1D boundary condition for $y\to 0$,

$$\psi(x,y)=f(x)\left(1-\frac{|y|}{a_{aa}}\right), \tag{6.3}$$

obtained by projecting Eq. (2.4) to the lowest transverse state. One finally obtains, after some algebra and the rescaling $\bar{k}=(\sqrt{3}/2\,a_{aa})\bar{u}$, the integral equation

$$\left[\frac{1}{\sqrt{1+3(u^2-\bar{u}^2)/4}}-1\right]f(u) \\ =-\frac{2}{\pi}\int_{-\infty}^{\infty}\frac{du' f(u')}{1+u^2+u'^2+uu'-3\bar{u}^2/4}, \tag{6.4}$$

which can also be obtained from the integral equation (5.7) in the BCS limit, i.e., from the scattering approach. For fermions, the same line of reasoning can be followed, and one obtains the integral equation (6.4) with an overall factor $-1/2$ factor on the right hand side. We conclude that the direct solution of Eq. (6.1) can provide exact results in the BCS limit for a_{ad}, b_{ad}, and possible trimer bound states.

A. Bosonic case

Equation (6.1) can be solved by using the Bethe Ansatz. The corresponding bosonic three-body wavefunction is written in the fundamental domain $\mathcal{D}_1 = \{z_1<z_2<z_3\}$ as

$$\psi(z_1,z_2,z_3)=\mathcal{N}\sum_P A(P)\,e^{i\sum_{j=1}^{3} z_j k_{Pj}}, \tag{6.5}$$

where $\mathcal{N}$ is a normalization constant, and the sum extends over all permutations of $\{1,2,3\}$, with coefficients [29]

$$A(P)=\prod_{1\leq j<l\leq 3}\left(1+\frac{2i/a_{aa}}{k_{Pl}-k_{Pj}}\right). \tag{6.6}$$

In other domains, the wavefunction is recovered by symmetry arguments. There is only one trimer bound-state solution [46, 47],

$$\psi(z_1,z_2,z_3)=\mathcal{N}\exp\left[-2(z_3-z_1)/a_{aa}\right], \tag{6.7}$$

here given in the fundamental domain $\mathcal{D}_1$, or in general form by Eq. (5.31). Using the boundary condition (6.3), we find that $f(u)=1/(u^2+4)$ solves Eq. (6.4) with $\bar{u}=iu_0=2i$, as discussed in Sec. V B.

We now turn to the atom-dimer scattering problem, putting $a_{aa}k_1=\bar{u}$, $a_{aa}k_2=-i-\bar{u}/2$ and $a_{aa}k_3=i-\bar{u}/2$, with the corresponding total energy

$$E=\frac{\hbar^2}{m_0\,a_{aa}^2}\left[-1+\frac{3}{4}\,\bar{u}^2\right], \tag{6.8}$$

see Eq. (3.3) in the BCS limit. From Eq. (6.5), the three-boson wavefunction is explicitely given. Using then the 1D boundary condition (6.3), we find in real space after some algebra, up to an overall normalization constant,

$$f(x)=(2-3i\epsilon\bar{u})\left[-(2-i\epsilon\bar{u})e^{i\bar{u}x}+2(2+i\epsilon\bar{u})e^{-i\bar{u}x/2}e^{-|x|}\right], \tag{6.9}$$

where $\epsilon=\mathrm{sgn}(x)$, and we have performed the rescaling $\sqrt{3}x/2a_{aa}\to x$ in order to give the correct atom-dimer distance in units of a_{aa}. Remarkably, the atom-dimer scattering does not give any reflected wave. The atom just passes the dimer and only acquires a phase shift, without being actually backscattered. Consequently, one can neither use the scattering Ansatz (3.4) nor define a_{ad}

and b_{ad} as in Eq. (3.6). We therefore need a more general definition to take into account the reflectionless situation found in the BCS limit. From Eq. (6.9) and its counterpart with $\bar{u} \to -\bar{u}$, we can use a simple but convenient basis for the incoming waves. The symmetric (antisymmetric) state is taken as a plane wave $e^{i\bar{u}x}$ coming from the left plus a plane wave $e^{-i\bar{u}x}$ ($-e^{-i\bar{u}x}$) from the right. In that basis, the scattering process is described by the 2×2 scattering matrix [30]

$$\mathcal{S} \equiv \begin{pmatrix} -e^{i\delta_s(\bar{u})} & 0 \\ 0 & e^{i\delta_a(\bar{u})} \end{pmatrix} = \begin{pmatrix} t+r & 0 \\ 0 & t-r \end{pmatrix}, \qquad (6.10)$$

where r and t are again energy-dependent reflection and transmission coefficients that can be read off from Eq. (6.9). At low energy, after expanding in $\bar{k} = \bar{u}/a_{aa}$, the phases $\delta_{a,s}$ define two scattering lengths according to

$$\delta_s(\bar{k}) = -2\bar{k}\, a_{ad} + \mathcal{O}(\bar{k}^2), \quad \delta_a(\bar{k}) = 2\bar{k}\, b_{ad} + \mathcal{O}(\bar{k}^2). \qquad (6.11)$$

This definition is more general than Eq. (3.6) and reduces to it when the Ansatz (3.4) applies. We also observe that in general two scattering lengths are needed to completely describe an arbitrary scattering process in 1D.

Using Eq. (6.9), we find for this atom-dimer scattering problem the result $b_{ad} = -2a_{aa} = -1/\sqrt{\Omega_B}$. This agrees with the asymptotic result in Fig. 4 for the BCS limit. Furthermore, we find $a_{ad} = -\infty$, in accordance with the divergence $a_{ad} \propto -1/\Omega_B^{3/2}$, see Fig. 4. Finally, we infer analytical results from Eq. (6.9) for the integral equation (5.10) in the BCS limit. Switching to Fourier space and expanding f in $\bar{u}$ as $f(u) = f_0(u) + \bar{u} f_1(u)$, we find

$$f_0 = -\pi\delta(u) + \frac{2}{1+u^2}, \qquad (6.12)$$

$$f_1 = -\pi\delta'(u) + \frac{2}{u(1+u^2)^2}, \qquad (6.13)$$

where each of these functions satisfies Eq. (6.4) for $\bar{u} = 0$. Plugging f_1 into Eq. (6.4) for $\bar{u} = 0$, we confirm the asymptotic behavior $b_{ad} = -1/\sqrt{\Omega_B}$ in the BCS limit, see Eq. (5.22). Plugging f_0 into Eq. (6.4) for $\bar{u} = 0$, we obtain the solution (5.23) with $h(0) = 0$ for any finite a_{ad}. Therefore the condition $h(0) = -1$ implies $a_{ad} = -\infty$.

B. Fermionic case

We now consider the fermionic ($\uparrow\uparrow\downarrow$) three-body problem and solve it via the Bethe Ansatz. The Schrödinger equation is essentially Eq. (6.1) with the three δ-functions replaced by $\delta(z_1-z_2)+\delta(z_1-z_3)$. This equation does not lead to any trimer state. The Bethe Ansatz for fermions is slightly different from the one for bosons. The form Eq. (6.5) also applies to the fermionic case, but the coefficients $A(P)$ are not given by Eq. (6.6) anymore. Moreover, the fundamental domain $\mathcal{D}_1$ is not sufficient, and we need to know the wavefunction in one more domain [48], e.g., $\mathcal{D}_2 = \{z_2 < z_1 < z_3\}$. The wavefunction in other domains then follows by anti-symmetry properties.

To study atom-dimer scattering, we now consider the momenta $a_{aa}k_1 = -i-\bar{u}/2$, $a_{aa}k_2 = i-\bar{u}/2$, and $a_{aa}k_3 = \bar{u}$, with total energy (6.8). Imposing the fermionic antisymmetry and normalizability, the problem reduces to the determination of three variables $\alpha_{1,2,3}$. The wavefunction is given in $\mathcal{D}_1$ by

$$\psi_1(z_1,z_2,z_3) = e^{i(k_1z_1+k_3z_2+k_2z_3)} - e^{i(k_1z_1+k_2z_2+k_3z_3)}, \qquad (6.14)$$

and in $\mathcal{D}_2$ by

$$\psi_2(z_1,z_2,z_3) = \alpha_1 e^{i(k_3z_1+k_1z_2+k_2z_3)} + \alpha_2 e^{i(k_1z_1+k_3z_2+k_2z_3)} + \alpha_3 e^{i(k_2z_1+k_1z_2+k_3z_3)}. \qquad (6.15)$$

The variables α_i are then obtained by imposing boundary conditions for the wavefunction and its first derivative with respect to z_1 and z_2 at the boundary between $\mathcal{D}_1$ and $\mathcal{D}_2$, $\{z_1 = z_2 < z_3\}$. The result is $\alpha_1 = 1-\chi$, $\alpha_2 = \chi$ and $\alpha_3 = -1$, where

$$\chi = -\frac{2+3i\bar{u}}{2+3i\bar{u}}.$$

Once the wavefunction $\psi(z_1,z_2,z_3)$ is known, we can use the boundary condition (6.3) and the rescaling $\sqrt{3}x/2a_{aa} \to x$ to get

$$f(x) = \epsilon(2-3i\epsilon\bar{u})\left(e^{-i\bar{u}x/2}e^{-|x|} - e^{i\bar{u}x}\right), \qquad (6.16)$$

where again $\epsilon = \mathrm{sgn}(x)$. Similar to the bosonic case, for arbitrary $\bar{u}$, there is no reflected wave. The scattering only leads to a phase shift that goes to π at zero energy. This implies a transmission coefficient $t = -1$, in contrast to the bosonic result $t = 1$. This discrepancy originates from the antisymmetry of the fermionic wavefunction with respect to exchange of the two $\uparrow$ atoms. As has been discussed in Sec. III C, we obtain from Eq. (6.16) and the definition (6.11) that $a_{ad} = (3/2)a_{aa} = 0.75/\sqrt{\Omega_B}$, and $b_{ad} = +\infty$. These results confirm the asymptotic behaviors shown in Fig. 1 for the BCS limit.

Also in the fermionic case, we can obtain analytical results for the integral equation (3.11) in the BCS limit. We first Fourier transform Eq. (6.16). The lowest order in $\bar{u}$ gives

$$f_0(u) = \frac{i}{u(1+u^2)}. \qquad (6.17)$$

Plugged into the fermionic equivalent of (6.4) for $\bar{u} = 0$, one finds the zero mode responsible for the divergence of b_{ad}, see Sec. III C. More precisely, $h_0 = (-i)u^2 f_0(u)$ satisfies the imaginary part of Eq. (3.11) in the BCS limit. The next order in $\bar{u}$ cannot be taken directly, since the resulting integral in the fermionic equivalent of Eq. (6.4)

is not well-defined for $u \to 0$ and $\bar{u} \to 0$. Instead, we use that $f(u)$ has the following form

$$f(u) = f_0(u) + \frac{3}{2}\, i\pi\bar{u}\delta(u-\bar{u}) + i\Gamma(u,\bar{u})\left(\frac{1}{\bar{u}-u} + \frac{1}{u}\right), \tag{6.18}$$

where $\Gamma(u,\bar{u})$ is a regular function. We insert this expression into the fermionic equivalent of Eq. (6.4) and look at the $\bar{u} \to 0$ limit. After some algebra as in Sec. III A, we obtain

$$\begin{aligned} &\int_{-\infty}^{\infty} \frac{du'}{2\pi u'^2}[G(u,u')h(u') - G(u,0)h(0)] \\ &- \left(\frac{1}{\sqrt{1+3u^2/4}} - 1\right)\frac{h(u)}{2u^2} = \frac{3}{4}\frac{1}{1+u^2} \end{aligned} \tag{6.19}$$

with

$$h(u) = \Gamma(u,0) = -1 + \frac{u^2(2+u^2)}{(1+u^2)^2} = -\frac{1}{(1+u^2)^2} \tag{6.20}$$

and $G(u,u') = (1+u^2+u'^2+uu')^{-1}$. This shows explicitly that Eq. (6.20) is a solution to the real part of Eq. (3.11) in the BCS limit, with the expected asymptotic behavior $a_{ad}/a_\perp = 0.75/\sqrt{\Omega_B}$. Although the form (6.18) seems similar to the general Ansatz (3.4), it is different since there is no reflection in the BCS limit, and Eq. (3.4) cannot apply.

C. Reflectionless potential

We have seen above that the divergence of b_{ad} (a_{ad}) for fermions (bosons) in the BCS limit was due to the reflectionless character of the atom-dimer effective potential. We shall now generalize this idea and show that for 1D scattering processes of a particle by any (possibly non-local) symmetric potential, the following statements are equivalent: (i) there is a divergence of the 1D scattering length a_1 (the 'odd' scattering length b_1), (ii) the potential has a quasi-bound state with even (odd) parity precisely at zero energy, and (iii) there is no reflection at zero energy. The atom-dimer scattering problem in the BCS limit, where higher channels are negligible, is in fact equivalent to a 1D scattering problem with such an effective non-local potential [43]. Therefore, the considerations in this section directly lead to physical insights for the BCS limit. The fact that in our case the reflection coefficient is zero for *any* incoming energy is an additional feature that cannot be inferred from the behavior of a_1 and/or b_1.

Symmetric potentials imply the low-energy scattering properties [34]

$$t(\bar{k})|_{\bar{k}\to 0} = -\frac{2i\bar{k}}{\nu}, \quad r(0) = -1, \tag{6.21}$$

where $\bar{k}$ is the wavevector of the incoming plane wave, and $\nu \neq 0$ is a *real* parameter that depends on the potential. The incoming wave is then totally reflected at zero energy. There is only one exception to this general low-energy behavior, arising for potentials with $\nu = 0$. In that case, the limit $\bar{k} \to 0$ is different and characterized by

$$t(0) = t_o = \pm 1, \quad r(0) = r_o = 0, \tag{6.22}$$

corresponding to a reflectionless situation at zero energy. For very small but finite ν, Eq. (6.21) still holds, but the reflection and transmission amplitudes change on the scale of unity in a narrow momentum region $\bar{k} \sim \nu$. For $\bar{k} > \nu$ (but still smaller than all other momentum scales), Eq. (6.22) is reached, and the potential is effectively reflectionless. We now show that for $\nu = 0$, the conditions (i), (ii) and (iii) are satisfied and equivalent to each other, while for finite ν, strictly speaking, none of them holds.

We first observe from the general definitions of a_1 and b_1, see Eqs. (6.10) and (6.11), that Eq. (6.22) leads to the divergence of a_1 (b_1) for $t_o = 1$ ($t_o = -1$). For $\nu \neq 0$, a_1 and b_1 are finite so that (i) holds iff (iii) is true. The small-ν regime is also interesting to investigate. Using Eq. (6.21), we find that for $t(\bar{k} \sim \nu) = 1$ (-1), a_1 (b_1) diverges as $-2/\nu$. To see if there is a quasi-bound state at zero energy, we consider the asymptotic form of the wavefunction

$$\psi(x) = \begin{cases} e^{i\bar{k}x} + r(\bar{k})e^{-i\bar{k}x}, & x \to -\infty\,, \\ t(\bar{k})\, e^{i\bar{k}x}, & x \to +\infty\,, \end{cases} \tag{6.23}$$

for which we take $\bar{k} = 0$. If $\nu \neq 0$, Eq. (6.21) gives $\psi = 0$ in the asymptotic region. Since a quasi-bound state at zero energy can only be an extended state, we conclude that ψ vanishes identically in this case. Conversely for $\nu = 0$, we obtain $\psi(x) = 1$ for $x \to -\infty$ and $\psi(x) = t_o = \pm 1$ for $x \to +\infty$. This means that there is an extended quasi-bound state at zero energy. Its parity follows from the asymptotic behavior, and we find that it is even if $t_o = +1$ but odd for $t_o = -1$. This shows that (ii) and (iii), and hence also (i), are equivalent.

In our specific case, the zero energy mode is found by taking $\bar{u} \to 0$ in Eqs. (6.9) and (6.16). This leads to (again, $\epsilon = \mathrm{sgn}(x)$)

$$f_0(x) = \begin{cases} 4\left(2e^{-|x|} - 1\right), & \text{for bosons,} \\ 2\epsilon\left(e^{-|x|} - 1\right), & \text{for fermions,} \end{cases} \tag{6.24}$$

or Eqs. (6.12) and (6.17) in momentum space. Now $f_0(x)$ is an even (odd) function for bosons (fermions), corresponding to a divergence of a_1 (b_1), as expected from our discussion above.

To conclude, let us discuss the position of the quasi-bound state for large a_1 or b_1 by analyzing the poles of the scattering matrix $\mathcal{S}$ in Eq. (6.10). If a pole appears for the scattering amplitude $e^{i\delta_s(\bar{k})}$ $(e^{i\delta_a(\bar{k})})$, the corresponding bound state is even (odd). For large values of a_1, we can use the expansion (6.11), and the equation for the even bound state is given by

$$1 + i\bar{k}a_1 = 0. \tag{6.25}$$

Analytic continuation to the physical sheet $\bar{k} = i\kappa$ ($\kappa > 0$) gives a real bound state with $\kappa = 1/a_1$ for $a_1 > 0$, with energy $E_e = -\hbar^2/m_0 a_1^2$. However, for $a_1 < 0$, we find, by analytic continuation to the unphysical sheet $\bar{k} = -i\kappa$, a *virtual* bound state with positive energy $E_e = \hbar^2/m_0 a_1^2$. For the three-boson problem in the BCS limit, $a_{ad} \to -\infty$. Consequently, the virtual quasi-bound state here comes down to zero from positive energies, and thus never becomes a real bound state of the three bosons. It simply reaches zero energy in the BCS limit, leading to the divergence of a_1. The situation is similar for an odd bound state. With the expansion Eq. (6.11), we find the bound-state equation $1 - i\bar{k}b_1 = 0$, so that the same conclusions as above can be formulated, with just a sign difference for b_1. Concerning the three-fermion problem, the same scenario for the virtual bound state is encountered, since there $b_{ad} \to +\infty$ in the BCS limit.

VII. CONCLUSIONS

In this paper, we presented the results of our study of the three-body problem in a quasi-1D confinement. We define and calculate two different 1D atom-dimer scattering lengths, a_{ad} and b_{ad}, which are directly accessible in scattering experiments. Physically, a_{ad} reflects the low-energy properties of the scattering phase shift for a symmetric wave while b_{ad} is the equivalent for an antisymmetric wave. Both can be inferred from the energy dependence of the transmission and the reflection coefficients. Technically, we derive a system of integral equations for the 1D scattering amplitudes with different transverse channel indices. For the sake of simplicity, the above system is projected onto the transverse ground state. We solve the ground-state equation numerically in general and analytically in the dimer and BCS limits. Note that the dimer and the BCS limits each correspond to different approaches to the 3D problem ($|a| \ll a_\perp$). Therefore we have investigated in detail the role of the higher transverse channels in both cases.

In the dimer limit, indeed it turns out that the higher channels contribute on the same footing. Their role is described by the 3D equations derived previously [35]. Note that the definition of the 1D scattering length remains distinct from that of the 3D scattering length even in the dimer limit. We establish a simple analytic relation between the latter and a_{ad}, valid both for bosons and fermions. In this limit $b_{ad} \to 0$, indicating that atom-dimer scattering can be regarded as potential scattering with a short-range effective potential. The resulting a_{ad} is negative for fermions but positive for bosons pointing to the existence of the confinement-induced trimer state in the latter case. Indeed we find such a state from the bound-state equation for bosons. Its energy is independent of the bosonic regularization parameter R^* in the large R^* limit.

The BCS limit is even more interesting: we show that higher channels can always be neglected here as far as the low-energy scattering is concerned. We find that the scattering is described by the three-particle Bethe Ansatz equations, i.e., we are dealing with two-body contact interactions. Then atom-dimer scattering cannot be viewed as potential scattering anymore. Although an effective potential can be defined, it is non-local and not short-ranged [43]. Instead atom-dimer scattering is found to be reflectionless: a_{ad} diverges for bosons, while b_{ad} diverges for fermions. In fact the Bethe Ansatz equations remain applicable also for the N-body problem in the BCS limit.

We have found a novel confined-induced trimer state for bosons. We trace the trimer state numerically from the dimer to the BCS limit provided Efimov physics can be neglected. Specifically in the dimer limit, we have discussed the interplay between this confined trimer state and the usual Efimov bound states. The trimer state is unique, its energy is nearly universal, and it matches the known Bethe Ansatz three-particle bound state in the BCS limit.

Acknowledgments

We thank A. Komnik for discussions. This work was supported by the SFB TR12 of the DFG.

APPENDIX A

We show here how to obtain the integral representation Eq. (1.6) from the more standard expression (see Ref. [49] for example)

$$\zeta(1/2,\Omega) = \lim_{N\to+\infty}\left(\sum_{n=0}^{N}\frac{1}{(n+\Omega)^{1/2}} - 2(N+\Omega)^{1/2}\right). \tag{A1}$$

We define $A_N = \left(\sum_{n=0}^{N}(n+\Omega)^{-1/2}\right) - 2\sqrt{N+\Omega}$ such that $\lim_{N\to+\infty} A_N = \zeta(1/2,\Omega)$. Using the integral representations

$$\frac{1}{\sqrt{n+\Omega}} = \int_0^\infty \frac{dt}{\sqrt{\pi t}} e^{-(n+\Omega)t},$$

$$\sqrt{N+\Omega} = \int_0^\infty \frac{dt}{\sqrt{\pi t}} \frac{1-e^{-(N+\Omega)t}}{t},$$

and the geometrical summation $\sum_{n=0}^{N} e^{-nt} = (1 - e^{-(N+1)t})/(1-e^{-t})$, A_N can be written as

$$\begin{aligned} A_N = &\int_0^\infty \frac{dt}{\sqrt{\pi t}}\left(\frac{e^{-\Omega t}}{1-e^{-t}} - \frac{1}{t}\right) \\ &+ \int_0^\infty \frac{dt}{\sqrt{\pi t}}\left(\frac{1}{t} - \frac{e^{-t}}{1-e^{-t}}\right) e^{-(N+\Omega)t}. \end{aligned} \tag{A2}$$

The second term in Eq. (A2) vanishes for large N so that we obtain the integral representation of Eq. (1.6).

[1] S. Jochim *et al.*, Science **302**, 2101 (2003); M. Greiner, C.A. Regal, and D.S. Jin, Nature (London) **426**, 537 (2003); M.W. Zwierlein *et al.*, Phys. Rev. Lett. **91**, 250401 (2003).

[2] C.A. Regal, M. Greiner, and D.S. Jin, Phys. Rev. Lett. **92**, 040403 (2004).

[3] M. Bartenstein *et al.*, Phys. Rev. Lett. **92**, 120401 (2004).

[4] M.W. Zwierlein *et al.*, Phys. Rev. Lett. **92**, 120403 (2004).

[5] T. Bourdel *et al.*, Phys. Rev. Lett. **93**, 050401 (2004).

[6] C. Chin *et al.*, Science **305**, 1128 (2004).

[7] M. Randeria, in *Bose-Einstein condensation*, ed. by A. Griffin, D.W. Snoke, and S. Stringari, p. 355 (Cambridge University Press, 1995).

[8] E. Timmermanns, P. Tommasini, M. Hussein, and A. Kerman, Phys. Rep. **315**, 199 (1999).

[9] Y. Ohashi and A. Griffin, Phys. Rev. Lett. **89**, 130402 (2002).

[10] R.A. Duine and H.T.C. Stoof, Phys. Rep. **396**, 115 (2004).

[11] A. Perali, P. Pieri, and G.C. Strinati, Phys. Rev. Lett. **93**, 100404 (2004).

[12] M. Holland, J. Park, and R. Walser, Phys. Rev. Lett. **86**, 1915 (2001).

[13] E.A. Donley, N.R. Claussen, S.T. Thompson, and C.E. Wieman, Nature **417**, 529 (2002).

[14] J. Herbig *et al.*, Science **301**, 1510 (2003).

[15] J.J. Hope and M.K. Olsen, Phys. Rev. Lett. **86**, 3220 (2000).

[16] M.G. Moore and A. Vardi, Phys. Rev. Lett. **88**, 160402 (2002).

[17] M. Olshanii, Phys. Rev. Lett. **81**, 938 (1998).

[18] T. Bergeman, M.G. Moore, and M. Olshanii, Phys. Rev. Lett. **91**, 163201 (2003).

[19] E. Braaten and H.W. Hammer, preprint cond-mat/0410417.

[20] I.V. Tokatly, Phys. Rev. Lett. **93**, 090405 (2004).

[21] J.N. Fuchs, A. Recati, and W. Zwerger, Phys. Rev. Lett. **93**, 090408 (2004).

[22] G.E. Astrakharchik, D. Blume, S. Giorgini, and B.E. Granger, Phys. Rev. Lett. **92**, 030402 (2004).

[23] A. Görlitz *et al.*, Phys. Rev. Lett. **87**, 130402 (2001).

[24] H. Moritz, T. Stöferle, M. Köhl, and T. Esslinger, Phys. Rev. Lett. **91**, 250402 (2003); T. Stöferle, H. Moritz, C. Schori, M. Köhl, and T. Esslinger, *ibid.* **92**, 130403 (2004).

[25] S. Richard *et al.*, Phys. Rev. Lett. **91**, 010405 (2003).

[26] B. Paredes *et al.*, Nature (London) **429**, 277 (2004).

[27] T. Kinoshita, T. Wenger, and D.S. Weiss, Science **305**, 112 (2004).

[28] A.O. Gogolin, A.A. Nersesyan, and A.M. Tsvelik, *Bosonization and Strongly Correlated Systems* (Cambridge University Press, 1998).

[29] M. Gaudin, *La fonction d'onde de Bethe* (Masson, 1983).

[30] B. Sutherland, *Beautiful models* (World Scientific, 2004).

[31] E. Nielsen, D.V. Fedorov, A.S. Jensen, and E. Garrido, Phys. Rep. **347**, 373 (2001).

[32] V. Peano, M. Thorwart, C. Mora, and R. Egger, cond-mat/0411517.

[33] K. Huang, *Statistical Mechanics* (Wiley, New York, 1987).

[34] L.D. Landau and E.M. Lifshitz, *Course of Theoretical Physics*, Vol.3 (Pergamon Press, 1980).

[35] G.V. Skorniakov and K.A. Ter-Martirosian, Zh. Eksp. Teor. Phys. **31**, 775 (1956) [Sov. Phys. JETP **4**, 648 (1957)].

[36] D.S. Petrov, Phys. Rev. A **67**, 010703(R) (2003).

[37] V.N. Efimov, Yad. Fiz. **12**, 1080 (1970) [Sov. J. Nucl. Phys. **12**, 589 (1971)]; Nucl. Phys. A **210**, 157 (1973).

[38] L.H. Thomas, Phys. Rev. **47**, 903 (1935).

[39] G.S. Danilov, Zh. Eksp. Teor. Phys. **40**, 498 (1961) [Sov. Phys. JETP **13**, 349 (1961)].

[40] R.A. Minlos and L.D. Faddeev, Zh. Eksp. Teor. Phys. **41**, 1850 (1961) [Sov. Phys. JETP **14**, 1315 (1962)].

[41] D.S. Petrov, Phys. Rev. Lett. **93**, 143201 (2004).

[42] D.S. Petrov, C. Salomon and G.V. Shlyapnikov, Phys. Rev. A **71**, 012708 (2005).

[43] C. Mora, R. Egger, A.O. Gogolin, and A. Komnik, Phys. Rev. Lett. **93**, 170403 (2004).

[44] E.H. Lieb and W. Liniger, Phys. Rev. **130**, 1605 (1963).

[45] M. Gaudin, Phys. Lett. **24 A**, 55 (1967); C.N. Yang, Phys. Rev. Lett. **19**, 1312 (1967).

[46] Y. Castin and C. Herzog, Compt. Rend. Acad. Sci. Paris, Ser. IV, **2**, 419 (2001).

[47] J.P. Straley, E.B. Kolomeisky, and S.C. Milne, J. Stat. Phys. **116**, 1579 (2004).

[48] M. Flicker and E.H. Lieb, Phys. Rev. **161**, 179 (1967).

[49] M.G. Moore, T. Bergeman, and M. Olshanii, J. Phys. IV France **116**, 69 (2004).